Redox Biology 54 (2022) 102392

Contents lists available at ScienceDirect

Redox Biology

journal homepage: www.elsevier.com/locate/redox

Dissecting the process of human neutrophil lineage determination by using alpha-lipoic acid inducing neutrophil deficiency model

Yong Dong [a,d,e,*,1], Yimeng Zhang [a,1], Yongping Zhang [b], Xu Pan [a], Ju Bai [a], Yijin Chen [a], Ya Zhou [a], Zhenyang Lai [c], Qiang Chen [a,c], Shaoyan Hu [b], Qiongxiu Zhou [a], Yonggang Zhang [a], Feng Ma [a,**]

[a] Center for Stem Cell Research and Application, Institute of Blood Transfusion, Chinese Academy of Medical Sciences & Peking Union Medical College (CAMS & PUMC), Chengdu, China
[b] Department of Hematology and Oncology, Children's Hospital of Soochow University, Suzhou City, China
[c] Sichuan Cord Blood Bank, Chengdu, China
[d] Department of Immunology, School of Basic Medical Sciences, Chengdu Medical College, Chengdu, China
[e] Non-coding RNA and Drug Discovery Key Laboratory of Sichuan Province, Chengdu Medical College, Chengdu, China

ARTICLE INFO

Keywords:
Alpha-lipoic acid
Neutrophils
Monocytes
ELK1
SF3B1
RNA splicing

ABSTRACT

Granulocyte-monocyte progenitors (GMPs) differentiate into both neutrophils and monocytes. Recently, uni-potential neutrophil progenitors have been identified both in mice and humans using an array of surface markers. However, how human GMPs commit to neutrophil progenitors and the regulatory mechanisms of fate determination remain incompletely understood. In the present study, we established a human neutrophil deficiency model using the small molecule alpha-lipoic acid. Using this neutrophil deficiency model, we determined that the neutrophil progenitor commitment process from CD371$^+$ CD115$^-$ GMPs defined by CD34 and CD15 and discovered that critical signals generated by RNA splicing and rRNA biogenesis regulate the process of early commitment for human early neutrophil progenitors derived from CD371$^+$ CD115$^-$ GMPs. These processes were elucidated by single-cell RNA sequencing both *in vitro* and *in vivo* derived cells. Sequentially, we identified that the transcription factor ELK1 is essential for human neutrophil lineage commitment using the alpha-lipoic acid (ALA)-inducing neutrophil deficiency model. Finally, we also revealed differential roles for long-ELK1 and short-ELK1, balanced by SF3B1, in the commitment process of neutrophil progenitors. Taken together, we discovered a novel function of ALA in regulating neutrophil lineage specification and identified that the SF3B1-ELK axis regulates the commitment of human neutrophil progenitors from CD371$^+$ CD115$^-$ GMPs.

1. Introduction

Neutropenia results in serious infection, fainting, low immunity, high fever, and chills. G-CSF injection is used to stimulate emergency granulopoieses for clinical treatment of neutropenia [1]. However, the application of G-CSF carries a significant risk of severe side effects, including spleen rupture, pulmonary toxicity, and other toxic reactions, so it is not suitable for the treatment of clinical neutropenia in all cases. As alternatives to G-CSF, neutrophil or granulocyte transfusion can also be used to treat neutropenia [2]. However, large numbers of neutrophils are required for clinical treatment, and the minimum transfusion dose is 1×10^9 cells/kg [3]. Meeting the neutrophil infusion dose is particularly challenging for patients with high body weight. Therefore, studying the regulatory molecular mechanisms of neutrophil lineage determination is critical for clinical neutrophil regeneration.

Granulocyte-monocyte progenitors (GMPs) are well-known to give rise to both monocytes and neutrophils. In humans, early neutrophil progenitors have been defined as Lin$^-$ CD66b$^{+/low}$ CD15^{low} CD49d$^+$ CD11b$^-$ [4] or Lin$^-$ CD66b$^+$ CD117$^+$ CD71$^+$ [5], and neutrophil committed progenitors are identified as CD66b$^-$CD64^{dim}CD115$^-$ in SSC^{low} CD45^{dim} CD34$^+$ and CD34$^{low/-}$ progenitors [6], but no uni-potential neutrophil progenitors have been identified within human

* Corresponding author. Huacai Road 26, Chengdu, China.
** Corresponding author. Huacai Road 26, Chengdu, China.
E-mail addresses: dong_yong@ibt.pumc.edu.cn (Y. Dong), mafeng@ibt.pumc.edu.cn (F. Ma).
[1] These authors as co-first authors.

https://doi.org/10.1016/j.redox.2022.102392
Received 30 May 2022; Received in revised form 27 June 2022; Accepted 29 June 2022
Available online 2 July 2022

GMPs by single-cell liquid culture [7]. However, how human common neutrophil progenitors commit from GMPs remains unknown [8]. Single-cell RNA sequencing and mass cytometry analyses cannot answer the neutrophil lineage commitment mechanism in detail [4,5]. Previous reports have demonstrated that post-transcriptional processes regulate the myeloblast-to-monocyte differentiation transition [9], megakaryocyte and erythrocyte lineages specification [10], and normal neutrophil differentiation [11]. Recently, the small molecule thymidine has been used to reprogram mouse fibroblast cells into neutrophils [12]. These studies suggest that commitment of neutrophil progenitors could also be controlled by RNA splicing. To elucidate the detailed mechanism of neutrophil progenitor fate determination, an inducible neutrophil differentiation model is required.

It is well known that antioxidants are commonly used to regulate cell proliferation and differentiation. The natural antioxidant ALA participates in metabolic regulation as a coenzyme in the TCA cycle [13] and regulates intracellular ROS levels [14]. ALA can be synthesized through the gene LIAS or ingested from food. Previous reports show that ALA can regulate cell proliferation and apoptosis through the ROS signaling pathway [15–17] and inhibit cancer progression [18–20]. Several studies show that alpha-lipoic acid (ALA) as one of the antioxidants can inhibit the differentiation and proliferation of hematopoietic stem progenitor cells (HSPCs) and maintains the function of hematopoietic stem cells (HSCs) both *in vivo* and *in vitro* [21–23]. As previous report shows that reactive oxygen species (ROS) play important role in mice emergency granulopoiesis [24]. Thus, we tried to explore the function of ALA in human neutrophil differentiation. In the present study, by adding ALA to the cell culture medium, we established an inducible neutrophil differentiation model from human cord blood $CD34^+$ HSPCs. Using this model, we determined how neutrophils differentiate from GMPs and elucidated the molecular mechanism of neutrophil progenitor commitment from GMPs. Additionally, we also confirmed that a similar commitment process of neutrophil progenitors occurs in human adult BM (bone marrow). Our findings suggested that the SF3B1-ELK1 signaling axis regulates early neutrophil commitment from $CD371^+$ $CD115^-$ GMPs via RNA splicing.

2. Materials and methods

2.1. Cell culture

To reveal the effect of antioxidants on multiple lineage differentiation, total cord blood nucleated cells or isolated $CD34^+$ cells were cultured in IMDM plus 10% FBS containing 8 cytokines (10 ng/mL SCF, 10 ng/mL FLT3L, 10 ng/mL TPO, 10 ng/mL IL-3, 10 ng/mL IL-6, 10 ng/mL GM-CSF, 20 ng/mL G-CSF and 2 U/mL EPO). Neutrophil and monocyte differentiation potential of indicated progenitors ($CD371^+$ GMPs, $CD371^-$ GMPs and $CD34^+$, $CD34^{low}$ or $CD34^-$ progenitors within the Lin^- $CD116^-$ $CD73^-$ $CD1c^-$ $CD115^-$ $CD123^{mid}$ $CD45RA^+$ $CD371^+$.) were sorted and cultured in IMDM plus 10% FBS containing 7 cytokines (10 ng/mL SCF, 10 ng/mL FLT3L 10 ng/mL TPO, 10 ng/mL IL-3, 10 ng/mL IL-6, 10 ng/mL GM-CSF and 20 ng/mL G-CSF). CD71 and GPA were used to indicate erythroid lineages, and CD15, CD66b, CD14 and CD11b were used to analyze neutrophils and monocytes.

To screen the antioxidants that affect human neutrophil differentiation, Alpha-lipoic acid (ALA) (Shanghai yuanye Bio-Technology Co., Ltd, #S26654) (25 μg/mL), L-Glutathione reduced (GSH) (MedChemExpress (MCE), #HY-D0187) (25 μg/mL), N-Acetyl-L-cysteine (NAC) (Sigma, #A9165-25G) (250 mM), N-Acetyl-D-cysteine (NAD) (MCE, #HY-136386)(250 mM), L-Ascorbic acid (MCE, # HY-B0166) (25 μg/mL), α-Vitamin E (MCE, #HY-N0683) (25 mM) and 1 mM H_2O_2 were added to the differentiation medium containing 7 cytokines from day0. ALA and NAC were dissolved in differentiation medium directly and stored at 4 °C for 3 weeks, while the GSG, NAD, L-Ascorbic acid and α-Vitamin E were dissolved and stored according to the manufacturer's instructions. To analyze the dose-effect of ALA on neutrophil differentiation, different doses (0.1, 0.5, 2.5, 10, 20, 50 μg/mL) of ALA were added to the 7-cytokine differentiation medium. Normally, we used 25 μg/mL ALA to analyze the effect of ALA on neutrophil differentiation for different hematopoietic progenitors.

Table 1
Target sequences for shRNAs.

shRNA Names	targets sequences
PRTN3_sh1	AGCTCAATGTCACCGTGGTCA
PRTN3_sh2	CCTGATCTGTGATGGCATCAT
PRTN3_sh3	CCTGACTTCTTCACGCGGGTA
LRG1_sh1	CATGCTGGACCTCTCCAATAA
LRG1_sh2	TGGACACCCTGGTATTGAAAG
LRG1_sh3	GCAATTAGAACGGCTACATCT
CEBPE_sh1	GCTGGAGTACATGGCAGAGAA
CEBPE_sh2	GCAAGAAGGCAGTGAACAAAG
CEBPE_sh3	CCTTTGCCTACCCTCCACATA
CLEC11A_sh1	CTGCCGGAACTGTTGAGGGAA
CLEC11A_sh2	GTGTCCTTCTTCGCCTGGCAT
CLEC11A_sh3	GCACTCCTCCTTGTTAGTGTC
KLF16_sh1	ACAAGTCCTCGCACCTAAAGTCG
E2F1_sh1	AGATCCCAGCCAGTCTCTACTCA
PBX3_sh1	ATGGACGATCAATCCAGGATGC
MYBL2_sh1	ACACAGATTCAGATGTGCCGGA
MLLT1_sh1	CAAAGTAGAGGAGTCGGGGTACG
ZDHHC13_sh1	CTCGCAGTGCAGGAATCACAGC
SNAPC4_sh1	GCACACAGAAAGAGCAGCTGAG
PBX1_sh1	TGATGAATCTCCTGCGAGAGCAA
SNRPB_sh1	CAGAAAGGGAAGAGAAGCGAGT
B3GAT3_sh1	CCCTTGCTGTTAGATAAGCCCA
SSBP4_sh1	GTGGAAACTCGATCCCCTACTC
HSF1_sh1	GCCATGAAGCATGAGAATGAGG
shRNA_ELK1_A	GCCTTGCGGTACTACTATGACA
shRNA_ELK1_L	CCAAACCTGAAATCGGAAGAGC
SF3B1_sh1	GCAGATTTGCTGGATACGTGAC
SF3B1_sh2	TGCTTTGATTTGGTGATGTAA
SF3B4_sh1	GACCAGTAGTCAACACCCACAT
SF3B4_sh2	CCCTGAGATTGATGAGAAGTT
SF3B5_sh1	GCCACTTCGACCTTCTCAACTA
SF3B5_sh2	TCCGCTTCAACTTGATGGAAA
SRSF3_sh1	GCATCGTGATTCCTGTCCATTG
SRSF3_sh2	TGGAACTGTCGAATGGTGAAA
SRSF11_sh1	GAGCTTTGATAGTCGTACCAT

To analyze the different effects of ALA on neutrophil differentiation derived from $CD34^+$HSPCs, we changed normal culture medium to the ALA containing medium at day2, day4, day6, day8 and day10, or conversely, replace the ALA medium with normal medium until day14. In ex vivo culture, higher percentage of $CD66b^+CD15^+CD14^-$ neutrophils are detected at day14 derived from $CD371^+CD115^-$ GMPs, and further culture will lead part of these cells to express CD14 ($CD66b^+CD15^+CD14^+$ neutrophils, APC like TANs [25]). To avoid unnecessary misunderstandings, flow cytometry is performed on day14.

2.2. ALA treatment of mice or hematopoietic stem/progenitor cells derived from mice BM

To analyze the effect of ALA on mice neutrophil differentiation *in vivo*. We intraperitoneally injected 2 mg ALA dissolved in 2.5%DMSO-corn oil [15] per-mice on every other day for 2 weeks, and 1 mg/mL ALA containing water was supplied every day at the same time. Flow cytometry assay was performed on day0 (before injection), day14 and day18 to detect $Ly6C^+$ $Ly6G^+$ neutrophils in peripheral blood.

To analyze the effect of ALA on mice neutrophil differentiation derived from Lin(CD2,CD3,CD4,CD8,Mac1,B220,Ter119) $^-$ $ckit^+$ $Sca1^+$ (LSK) in *ex-vivo* culture, we sorted LSK for *in vitro* differentiation using 8 cytokines (mSCF, mTOP, mG-CSG, mGM-CSG, mIL-3, mIL-6, hFLT3L, hEPO) containing medium ±25 μg/mL ALA. Flow cytometry assay was performed to analyze $Ly6C^+$ $Ly6G^+$ neutrophils at day5 day7 and day9. Finally, MGG (May-Grunwald Giemsa) stain was used to analyze the cell morphology of ALA treated cultures of not.

2.3. Cell morphology assay

Total cultures or sorted cells were centrifuged onto glass slides using a Cell Cytospin machine (Cytospin 4, Thermo Fisher Scientific), and MGG (May-Grunwald Giemsa) stain was used to analyze the cell morphology as previously reported [26].

2.4. Gene-expressing plasmid and shRNA-expressing plasmid construction

The cDNA of CLEC11A (NM_002975), LRG1 (NM_052 972), PRTN3 (NM_002777), CEBPE (NM_001805), CEBPE-M (U80982.1), XRCC3, TMEM176B, PBX3, MDM1, MDB3, HMGA1, ELK1, and short-ELK1 from the dsDNA of neutrophil biased progenitors was cloned into the PCCL-MND-PGK-dsRed or PCCL-MND-PGK-EGFP lentiviral vector as previously reported [27]. Knocking down the target genes in $CD34^+$ cells was mediated by short hairpin RNA (shRNA). All the plasmids (Plko.1-EGFP, Plko.1-PRTN3-shRNA1-EGFP, Plko.1-PRTN3-shRNA2-EGFP, Plko.1-PRTN3-shRNA3-EGFP, Plko.1-LRG1-shRNA1-EGFP, Plko.1-LRG1-shRNA2-EGFP, Plko.1-LRG1-shRNA3-EGFP, Plko.1-CLEC11A-shRNA1-EGFP, Plko.1- CLEC11A-shRNA2-EGFP and Plko.1-CLEC11A-shRNA3-EGFP were prepared by Feng Hui Sheng Wu, Co., Ltd. Three targeted sequences of each gene were inserted into the lentiviral expression vector Plko.1-EGFP-Puro (#FH1717, FENGHUISHENGWU Co., Ltd, China). In addition, the shRNA expression vectors of B3GAT3, ELK1, E2F1, HSF1, KLF16, MLLT1, MYBL2, SNRPB, SSBP4, TRIM28, and ZDHHC13 were cloned to analyze their function in neutrophil or monocyte differentiation. The target sequences are provided in Table 1.

2.5. Lentiviral transduction and neutrophil or monocyte differentiation potential assay

Lentiviral preparation and transduction of $CD34^+$ HSPCs were performed as we previously described [27]. The neutrophil and monocyte differentiation potential of total transduced cells or sorted transduced cells (GFP^+ $CD115^-$ $CD371^+$ gated $CD34^+$ $CD15^-$, $CD34^{mid}$ $CD15^{mid}$, $CD34^{low/-}$ $CD15^+$) was analyzed by culturing in IMDM plus 10% FBS containing 7 cytokines (10 ng/mL SCF, 10 ng/mL FLT3L, 10 ng/mL TPO, 10 ng/mL IL-3, 10 ng/mL IL-6, 10 ng/mL GM-CSF and 20 ng/mL G-CSF) for 7–14 days.

2.6. Bulk cell RNA-seq

Two thousand $CD371^+CD115^-$ GMP, $CD34^{mid}CD115^+$MoP, NbP1, NbP2 and NbP3 cells derived from cultures or BM were sorted into 1.5 mL tube containing 200 μL 0.5% BSA-DPBS solution. The dsDNA and libraries were generated as previously described. And all the libraries were sequenced using the Illumina NovaSeq6000 system (Novogene Co., Ltd.). The clean fastq data were aligned to the hg38 human genome using Hisat2. R packages of DESeq2, ggplots clusterProfiler and GSEA were used to analyze the differentially expressed genes and gene ontology enrichment and gene set enrichment.

To assay the signals changing under the overexpression of L-ELK1 and S-ELK1, we sorted two thousand NbP1 derived from L-ELK1 and S-ELK1 transduced $CD34^+$ HSPCs to generate DNA libraries as previously described. Data analysis was performed as described above.

2.7. In vitro single-cell RNA-seq analysis

To reveal the *in vitro* transcriptome characteristics of neutrophil differentiation at different stages at the single cells level, we sorted the $CD371^+$ $CD115^-$ GMPs, $CD115^+$ $CD34^{mid}$ MoPs, $CD115^-CD34^{mid}$ $CD371^+$ early neutrophil biased progenitors (ENbPs), $CD115^-$ $CD34^{low}$ $CD371^+$ late neutrophil biased progenitors (LNbPs) $CD371^+$ $CD66b^-$, and $CD371^+$ $CD66b^+$ cells for single cell RNA-Seq and the double-strand cDNA library of single cells was generated as previously reported [28]. The quality control of amplified cDNA was analyzed by RT-PCR analysis of the housekeeping gene B2M. Samples with CT values less than 25 were used for sequencing library preparation using Vazyme TruePrepTM DNA Library Prep Kit V2 from Illumina (Vazyme, TD-503). Library sequencing was performed using the Illumina NovaSeq 6000 system (Novogene Co., Ltd.).

All fastq files were mapped to the human hg38 genome by HISAT2 software, and raw count data were calculated using featureCounts software. For bulk cell RNA-seq, the DESeq2 package was used to normalize the raw data and determine the differentially expressed genes. For the single-cell RNA-seq data, all the raw count data were normalized by transforming into CPM (counts per million) values by the edgeR program. Unsupervised cluster analysis was performed to evaluate the accuracy of sorted cells. In total, 165 single cells (40 $CD371^+$ $CD115^-$ GMPs, 24 $CD115^+$ $CD34^{mid}$ MoPs, 29 $CD115^-CD34^{mid}$ $CD371^+$ early neutrophil biased progenitors (ENbPs), 34 $CD115^-$ $CD34^{low}$ $CD371^+$ late neutrophil biased progenitors (LNbPs), 18 $CD371^+$ $CD66b^-$, and 20 $CD371^+$ $CD66b^+$ cells) were retained for further analysis. Multiple t-tests were used to identify the statistically significant differentially expressed genes for different cell groups. PCA and the UMAP method were used to analyze the single-cell RNA, and Monocle was used to perform the cell trajectory interference.

The R packages sincell, pcaMethods, uwot, gplots, clusterProfiler, and reshape2 were used to analyze the single-cell data. The DESeq2, clusterProfiler, and GSEA packages were used to analyze the differentially expressed genes, GO enrichment, and pathways for bulk cell RNA-seq data.

2.8. 10x single-cell RNA-seq of BM derived cells

To dissect the *in vivo* transcriptome characteristics of neutrophil lineage cells at different stages, 10 000 Lin/CD116/CD1C/$CD73^-$ $CD371^+$ $CD123^+$ cells derived from human adult BM of two healthy donors were sorted for droplet-based cell harvest by a 10X Genomics Chromium system. The fastq raw files were processed by Cell Ranger 4.0.4 software to obtain the gene expression matrix. Cells with more than 2500 detected genes (an average of 4500 genes were detected) were used to perform further clustering. To further define the populations, we used CD1c, CD1d, CCR6, and CLEC10A to define dendritic progenitor cells, HOXA9, HOXA10, HOXB4, and CD34 to define $CD371^+$ GMPs, CD34, MPO, PRTN3, ELANE, and CLEC11A to define neutrophil biased progenitors, and CD115 (CSF1R), MAFB, MAFF, and CD14 to define monocyte progenitors. Finally, Monocle2 was used to determine the cell trajectory of $CD371^+$ GMPs, neutrophil biased progenitors and monocyte progenitors. Fastq files or processed data were uploaded to the Gene Expression Omnibus public database (GSE184864).

2.9. Immunofluorescence staining

Sorted cells were centrifuged onto glass slides using a Cell Cytospin machine (Cytospin 4, Thermo Fisher Scientific), and cells were fixed using 4% paraformaldehyde in PBS pH 7.4 for 10 min at room temperature. The fixed cells were washed three times with cold PBS and then permeabilized using 0.2% Triton X-100 for 10 min at room temperature. The cells were gently washed with PBS three times. The cells were blocked with 1% BSA for 30 min and then incubated with 1:50 diluted primary antibodies (anti-ELK1 N-terminus antibody (Biorbyt, orb213892, indicates S-ELK1 and L-ELK1) and anti-ELK1 C-terminus antibodies (Affinity, AF6212, only indicates the L-ELK1)) in 1% BSA overnight at 4 °C. The cells were gently washed with cold PBS three times. The cells were incubated with goat IgG (H + L) cross-adsorbed secondary antibody Alexa Fluor ® 555 conjugate antibody (Thermo-Fisher, A-21432)) for 1 h at room temperature. The secondary antibody solution was decanted and washed three times for 5 min. Finally, the cells were incubated with 1 μg/mL Hoechst3342 for 1 min. The pictures were harvested by a confocal microscope LSM900 with the same parameters.

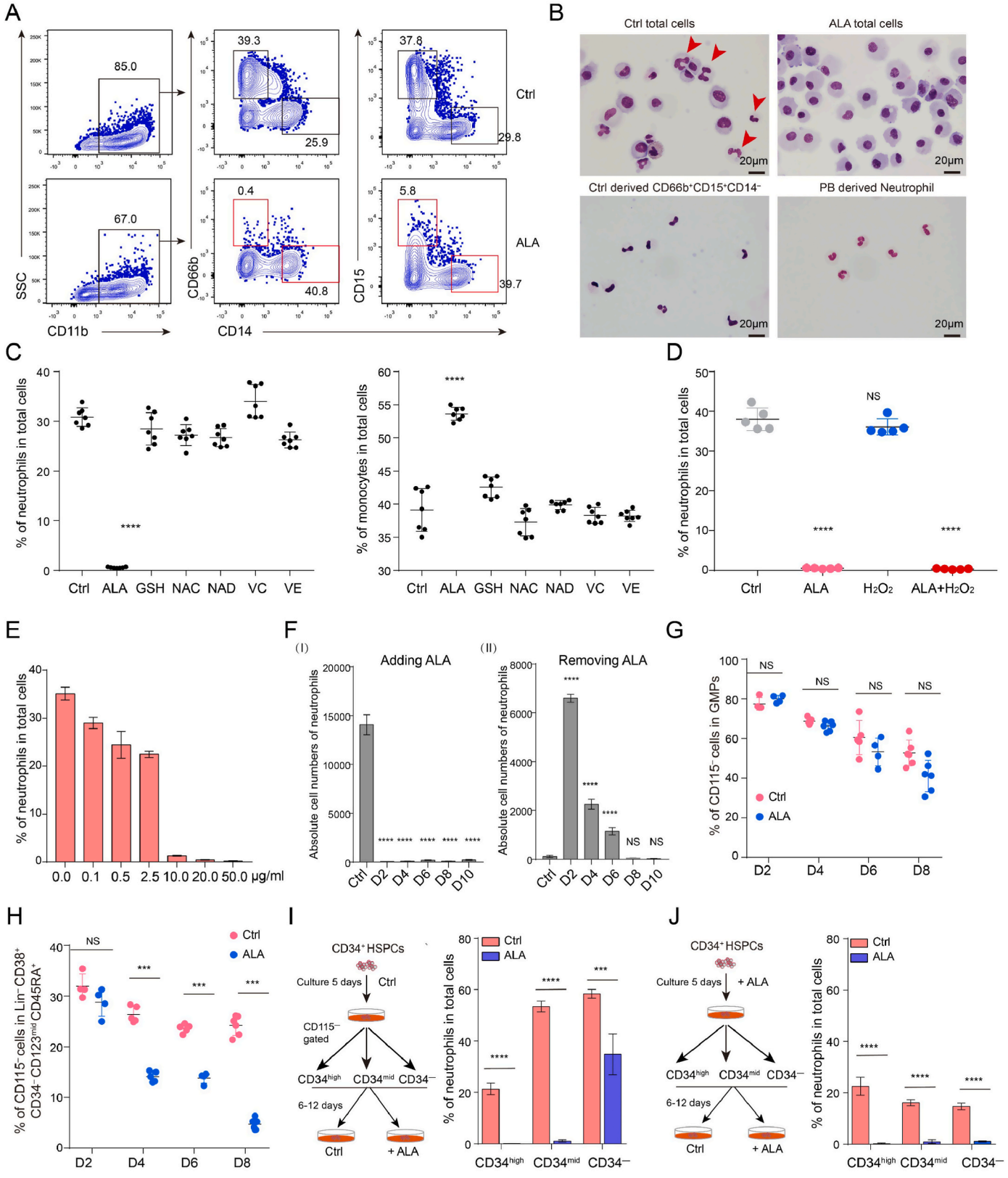

(caption on next page)

Fig. 1. ALA impedes human neutrophil commitment.
(A) Representative flow cytometry plots of $CD11b^+$ $CD66b^+$ $CD15^+$ $CD14^-$ neutrophils and $CD11b^+$ $CD14^+$ $CD66b^-$ $CD15^-$ monocytes derived from $CD34^+$ HSPCs of CB ± ALA. Flow cytometry was performed on day 14 of culture.
(B) MGG staining assay to determine the morphology of Ctrl cultures, ALA-treated cultures, and $CD66b^+$ $CD15^+$ $CD14^-$ neutrophils derived from Ctrl cultures and peripheral blood. Scale bar = 20 μm **(C)** Percentages of $CD11b^+$ $CD66b^+$ $CD15^+$ $CD14^-$ neutrophils and $CD11b^+$ $CD14^+$ $CD66b^-$ $CD15^-$ monocytes derived from cord blood $CD34^+$ hematopoietic stem/progenitor cells (HSPCs) treated with different antioxidants (Alpha-lipoic acid = ALA, L-Glutathione reduced = GSH, N-Acetyl-L-Cysteine = NAC, N-Acetyl-D-cysteine = NAD, L-Ascorbic acid = VC, α-Vitamin E = VE). Flow cytometry was performed to measure neutrophil and monocyte percentages on day 14 of culture.
(D) Statistical analysis of neutrophil percentages in total cells derived from $CD34^+$ HSPCs ± ALA or H_2O_2 treatment.
(E) Statistical analysis of neutrophil percentages derived from $CD34^+$ HSPCs with different doses of ALA (0.1, 0.5, 2.5, 10, 20, 50 μg/mL).
(F) Absolute cell number of neutrophils derived from $CD34^+$ HSPCs under 20 μg/mL ALA treatment at different days. ALA was added to (I) and removed from (II) culture medium at day 2 (D2), day 4 (D4), day 6 (D6), day 8 (D8), and day 10 (D10). Flow cytometry was performed on day14. The Ctrl for addition of ALA was the absence of ALA, and the Ctrl for removing ALA was treatment for the duration of the experiment.
(G–H) Proportion of $CD115^-$ cells in Lin^- $CD38^+$ $CD34^+$ $CD123^+$ $CD45RA^+$ GMPs and Lin^- $CD38^+$ $CD34^-CD123^+$ $CD45RA^+$. $CD34^+$ HSPCs were cultured ± ALA treatment. Flow cytometry analysis of $CD115^-$ cells in the indicated populations was performed on day 2 (D2), day 4 (D4), day 6 (D6), or day 8 (D8).
(I–J) Percentages of neutrophils derived from $CD34^+$, $CD34^{low}$, or $CD34^-$ cells within $CD115^-$ cells at day 5 culture with ALA treatment (J) or vehicle treatment (I). Sorted $CD115^-$ $CD34^+$, $CD115^-$ $CD34^{low}$, or $CD115^-$ $CD34^-$ cells were cultured ± ALA treatment for 6–12 days and flow cytometry assay was performed to analyze $CD11b^+$ $CD66b^+$ $CD15^+$ $CD14^-$ neutrophils and $CD11b^+$ $CD14^+$ $CD66b^-$ $CD15^-$ monocytes.
Data of **(C–I)** are expressed as means ± SD. Each symbol in **(C, D, G, H)** represents an individual replicate, and small horizontal lines indicate the mean (±SD.). An unpaired Student's *t*-test (two-tailed) was performed to evaluate statistical significance. NS = not significant, *P < 0.05, **P < 0.01, ***P < 0.001, ****P < 0.0001, N = 3–7.

2.10. RNA-protein interaction assay

RNA pull-down and immunoblotting were performed to assay the interaction of SF3B1 and ELK1 mRNA. According to the absent sequence of S-ELK1 compared to L-ELK1, we synthesized 5′-biotin-modified RNA (20 bp) around the splicing site. RNA pulldown and immunoblotting were performed as previously described [29,30]. In brief, 1 mol of each biotin-modified RNA was added to the washed agarose beads, incubated at 4 °C for 3–4 h with 180 U/mL RNase inhibitor (Biosystems, AM2694) and resuspended in 500 μL of RNA-streptavidin interaction buffer after washing twice. Cellular nuclear proteins were extracted by a Nuclear and Cytoplasmic Protein Extraction Kit (Beyotime), and then 100 μL was added to an agarose-streptavidin-biotin-RNA tube and incubated at 4 °C overnight under 100–150 RPM rotation. After this procedure, 15 μL SDT buffer (2% SDS, 100 mM DTT, 100 mM Tris-HCl, pH = 7.6) was added to the pellets and incubated at 95 °C for 5 min to elute the proteins after washing twice with the interaction buffer. The supernatant liquid was used as the input for the mass spectrometry assay (Performed by Aptbiotech. Ltd.) to identify the proteins binding to ELK1 biotin-RNA.

2.11. Humanized immunodeficient mouse transplantation

L-ELK1-, S-ELK1-, ELK1-shRNA-A (target to all transcripts)- and ELK1-shRNA-L (target to only the long coding protein transcript)-transduced $CD34^+$ HSPCs were transplanted into B-NDG-SM humanized immunodeficient mice expressing human SCF and GM-CSF purchased from Beijing Biocytogen Co., Ltd. Transplantation was conducted as previously reported [21]. To improve neutrophil differentiation, 100 ng/mL human IL-3 and G-CSF were injected into mice plus cells. Flow cytometry assay was performed on day18 after transplantation. All animal experiments were approved by the Institutional Ethics Review Committee of Institute of Blood Transfusion (IERC-IBT).

2.12. Statistical analysis

The R packages of edgeR, DESeq2, clusterProfiler, pcaMethods, gplots, reshape2, ggplot2, Seurat, monocle2, GSEA, cluster, factoextra, uwot and sincell were used to perform statistical analysis of RNA-Seq data. Other significant analyses were performed using unpaired Student's t-tests (GraphPad Prism, GraphPad Software).

2.13. Data availability

The data that support the findings of this study are available from the corresponding author upon request. All RNA-Seq data are deposited in the GEO database with accession code GSE184864.

3. Results

3.1. ALA impedes human neutrophil commitment

Our previous report shows that ALA is helpful to maintain the stemness of hematopoietic stem cells [21]. To determine the function of ALA on blood cell lineage differentiation, CB $CD34^+$ hematopoietic stem/progenitor cells (HSPCs) were sorted and cultured in 10% fetal bovine serum (FBS) IMDM medium containing SCF, FLT3L, IL-3, IL-6, TPO, GM-CSF, G-CSF and EPO ± ALA. Surprisingly, ALA completely inhibited production of $CD11b^+$ $CD14^-$ $CD66b^+$ $CD15^+$ neutrophils and increased $CD11b^+$ $CD14^+$ $CD66b^-$ $CD15^-$ monocytes production (Fig. 1. A). Morphological analysis also demonstrated that ALA blocked generation of $CD11b^+$ $CD66b^+$ $CD15^+$ polymorphonuclear neutrophils (PMNs) (Fig. 1. B) We also determined the effect of ALA on $CD66b^+$ $CD14^-$ and $CD66b^-$ $CD14^-$ populations. ALA did not block the cell proliferation of $CD66b^+$ $CD15^+$ neutrophils. Although ROS are reported to be related to emergency granulopoiesis [24], we contend that ROS are not sufficient to control neutrophil commitment. Thus, we postulated that ALA inhibition of neutrophil differentiation was unlikely to be related to its antioxidant function, but rather by other unknown functions. To test this hypothesis, we added 1 mM H_2O_2 and commonly used antioxidants that could scavenge ROS in $CD34^+$ HSPCs (Supplementary Fig. 1. A), including N-Acetyl-L-Cysteine (NAC), N-Acetyl-D-cysteine (NAD), L-Glutathione reduced (GSH), α-Vitamin E ((+)-α-Tocopherol), and L-Ascorbic acid (Vitamin C) to the culture medium ± ALA. Neither H_2O_2 nor other antioxidants (GSH, NAC, NAD, α-Vitamin E and Vitamin C) treatment affected the production of neutrophils and monocytes (Fig. 1 C-D), indicating that ALA inhibited human neutrophil differentiation independently of its effects on ROS. Additionally, ALA did not block neutrophil differentiation from Lin (CD2, CD3, CD4, CD8, B220, Mac1, Ter119)$^-$ c-kit$^+$ sca1$^+$ mouse HSPCs (Supplementary figure 1 B-D).

Furthermore, we determined the dose-dependent effect of ALA on $CD34^+$ HSPC differentiation. ALA had a dose-dependent effect on neutrophil differentiation of $CD34^+$ HSPCs, and 20 μg/mL of ALA completely inhibited neutrophil production (Fig. 1. E). To determine the stage at which ALA blocks neutrophil differentiation, $CD34^+$ HSPCs were sorted and cultured ± ALA treatment. ALA was added to or removed from culture medium at different time points, and flow cytometry analysis was performed on day 14. Both the addition and removal of ALA hindered neutrophil differentiation (Fig. 1. F). We thus postulated that ALA impaired the commitment of neutrophil

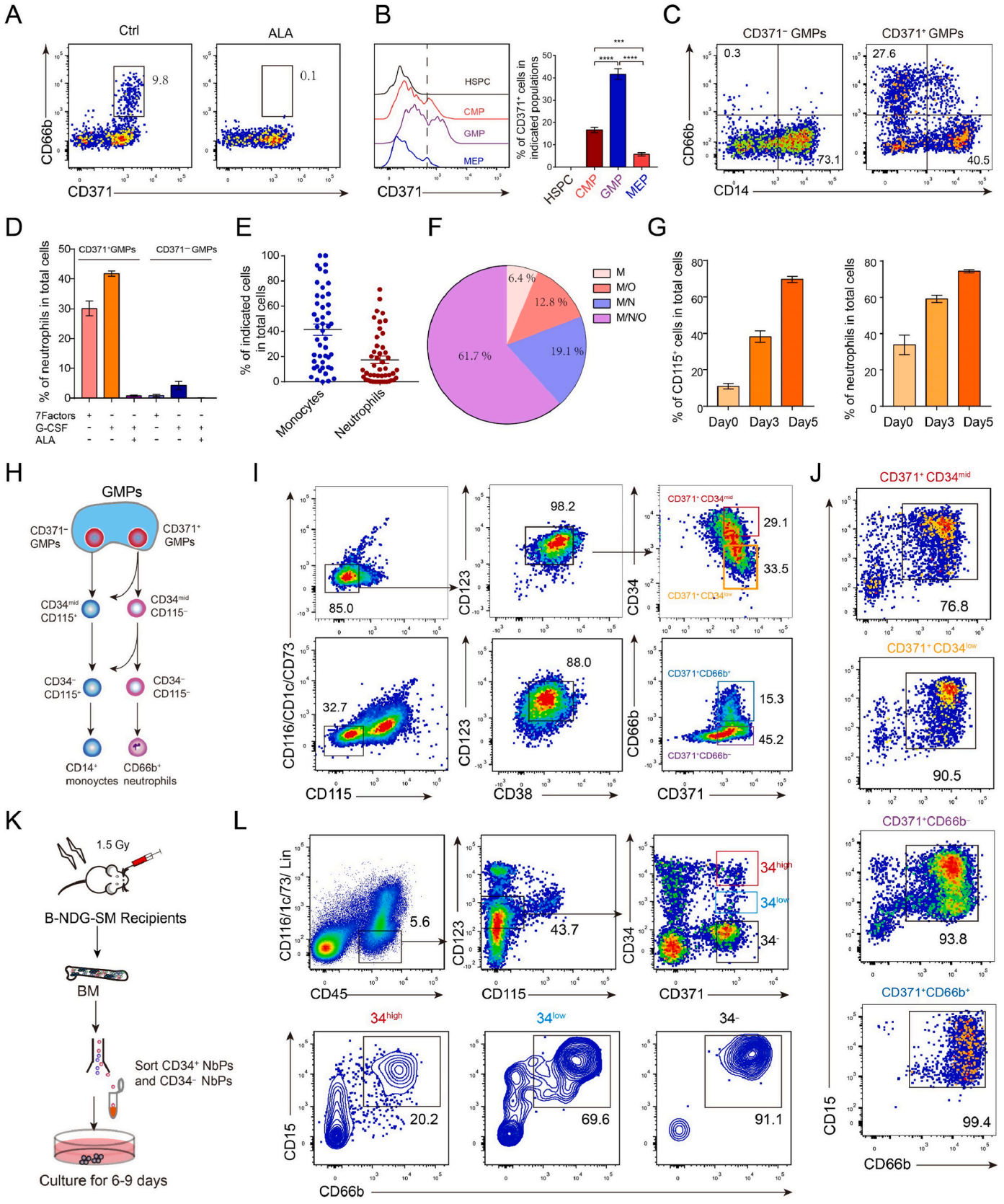

(caption on next page)

Fig. 2. Human neutrophils are derived from CD115$^-$CD371$^+$ GMPs.
(A) Representative flow cytometry plots of CD66b$^+$ neutrophils within CD371$^+$ cells derived from CB CD34$^+$ HSPCs ± ALA. Flow cytometry was performed at day 9.
(B) Flow cytometry analysis of the proportion of CD371$^+$ progenitors in Lin$^-$ CD38$^-$ CD34$^+$HSPCs, Lin$^-$ CD38$^+$ CD34$^+$ CD123^{mid} CD45RA$^-$ CMPs (common myeloid progenitors), Lin$^-$ CD38$^+$ CD34$^+$ CD123^{mid} CD45RA$^+$ GMPs and Lin$^-$ CD38$^+$ CD34$^+$ CD123$^-$ CD45RA$^-$ MEPs (megakaryocyte-erythroid progenitors) ± ALA.
(C) Representative flow cytometry plots of CD11b$^+$CD66b$^+$CD14$^-$neutrophils and CD11b$^+$CD66b$^-$CD14$^+$ monocytes derived from CD371$^-$ GMPs and CD371$^+$ GMPs.
(D) Neutrophil production in CD371$^+$ GMPs and CD371$^-$ GMPs under the specified treatments, including culture with seven cytokines, G-CSF only, or G-CSF and ALA. Flow cytometry assay to performed to analyze the CD11b$^+$CD15$^+$CD66b$^+$CD14$^-$ neutrophils in total cells at day14 of culture.
(E) Single-cell assay for the neutrophil and monocyte differentiation potentials of CD371$^+$ GMPs.
(F) Pie diagram illustrating percentages of progenitors with different lineages (M: monocyte, N: neutrophil, O: others).
(G) Neutrophil differentiation potential of CD115$^-$ progenitors derived from CD371$^+$ GMPs at different time points. Percentages of CD115$^+$ progenitors and neutrophils derived from CD115$^-$ progenitors are shown.
(H) Conjecture model diagram of neutrophil and monocyte differentiation derived from GMPs.
(I) Representative flow cytometry plots of the sorting gate for neutrophil-biased progenitors derived from CD115$^-$CD371$^+$ GMPs at day 3 and day 6.
(J) Flow cytometry analysis of the neutrophils from sorted CD371$^+$ CD34^{high}, CD371$^+$ CD34^{mid} (day 3), CD371$^+$ CD66b$^-$ and CD371$^+$CD66b$^+$ (day 6) cells derived from CD115$^-$ CD371$^+$ GMPs from day 6 to day 9.
(K) *In vivo* experimental strategy to analyze neutrophil-biased progenitors from B-NDG-SM mouse BM.
(L) Flow cytometry analysis of the neutrophil differentiation potential of sorted neutrophil-biased progenitors from B-NDG-SM mouse BM at day 6–day 9. Data in **(B, D, E, G)** are represented as means ± SD. Each symbol of **(E)** represents one cell, and small horizontal lines indicate the mean (±SEM.). An unpaired Student's *t*-test (two-tailed) was performed to assess statistical significance. ***P < 0.001, ***P < 0.0001.

progenitors. Given that neutrophils are mainly derived from CD115$^-$ populations [31], we analyzed the CD115$^-$ GMP-like cells and CD115$^-$ CD34$^-$ CD123^{mid} CD45RA$^+$ CD38$^+$ progenitors on day 2, day 4, day 6, and day 8. CD34$^-$ CD115$^-$ CD123^{mid} CD45RA$^+$ CD38$^+$ progenitors, but not the CD115$^-$ GMP-like cells, were significantly decreased on day 4, day 6, and day 8 with ALA treatment (Fig. 1G-H). Finally, to determine which stages does ALA block neutrophil differentiation, we sorted CD115$^-$ CD34$^+$, CD115$^-$ CD34^{mid}, and CD115$^-$ CD34$^-$ cells derived from Ctrl cultures for continuous differentiation culture. A higher proportion of neutrophils were detected in CD115$^-$ CD34$^-$ progenitors derived cultures compared to CD115$^-$ CD34$^+$, CD115$^-$ CD34^{mid} progenitors, and ALA completely blocked neutrophil differentiation of CD34^{high} and CD34^{mid} progenitors, but not in CD34$^-$ progenitors (Fig. 1. I). Furthermore, CD115$^-$ CD34$^+$, CD115$^-$ CD34^{mid}, and CD115$^-$ CD34$^-$ progenitors derived from ALA treated cultures at day5 were sorted for continuous culture. Almost no neutrophils were detected in CD34^{high} CD34^{mid} and CD34$^-$ progenitors with continuous ALA treatment (Fig. 1. J). A significantly lower proportion of neutrophils were detected from ALA-treated CD115$^-$ CD34^{mid} (16.17 ± 1.2%) compared to Ctrl culture-derived CD115$^-$ CD34^{mid} (53.4 ± 2.1%), and ALA-treated CD115$^-$ CD34$^-$ (14.7 ± 1.3%) progenitors compared to culture-derived CD115$^-$ CD34$^-$ (58.4 ± 1.8%). but not for CD115$^-$ CD34^{high} progenitors (Fig. 1 I-J)). Together, these findings indicated that neutrophil progenitors commit to the neutrophil fate concomitant with decreasing CD34 expression, and that ALA impedes the commitment of neutrophil progenitors.

3.2. CD371$^+$ GMPs commit to neutrophil progenitors by losing monocyte differentiation potential

In prior studies, single-cell culture of human GMPs revealed that cells differentiated from the culture were neutrophils, but that this is accompanied by a small amount of monocyte production [7], indicating that human neutrophil progenitor fate determination could occur downstream of GMP differentiation. However, the ways by which neutrophil progenitors are committed from GMPs remains unknown. Prior reports have indicated that almost all CFU-G colonies or CD66b$^+$ granulocytes are derived from CD64$^{mid/-}$CD371$^+$ GMPs [32] excluding the CD115$^+$ cells [6]. Therefore, to confirm that CD66b$^+$ neutrophils were derived from CD371$^+$ progenitor cells, we performed flow cytometry analysis to measure the neutrophils at day 7 of *in vitro* differentiation of CB-derived GMPs. Only CD371$^+$ cells produced CD66b$^+$ neutrophils and ALA blockage of CD371$^+$ cells gave rise to CD66b$^+$ neutrophils (Fig. 2. A). Flow cytometric analysis of CD34$^+$ CD38$^-$ HSPCs, CD34$^+$ CD38$^+$ CD123^{mid} CD45RA$^-$ CMPs (Common myeloid progenitors, CMPs), CD34$^+$ CD38$^+$ CD123^{mid} CD45RA$^+$ GMPs, and CD34$^+$ CD38$^+$ CD123$^-$ CD45RA$^-$ MEPs (Megakaryocyte-erythroid progenitor cell, MEPs) demonstrated that GMPs contained a higher proportion of CD371$^+$ progenitor cells (Fig. 2. B). To determine the neutrophil differentiation potential of CD371$^+$ progenitors, we sorted CD371$^+$ GMPs and CD371$^-$ GMPs for neutrophil differentiation, revealing that neutrophils are mainly derived from CD371$^+$ GMPs, but not CD371$^-$ GMPs (Fig. 2. C). Furthermore, ALA completely blocked the differentiation of CD371$^+$GMPs into neutrophils, even under treatment with G-CSF only (Fig. 2. D). To further analyze the neutrophil differentiation potential of CD371$^+$ GMPs, we sorted CD371$^+$ GMPs for single-cell differentiation analysis. CD371$^+$ GMPs contained no committed neutrophil progenitors, except monocyte progenitors (Fig. 2 E-F), and CD371$^+$ GMPs contained different neutrophil differentiation potential progenitors (Fig. 2E-F). In addition, flow cytometry analysis revealed that CD371$^+$ GMPs contained CD115^{low} cells (Supplementary Fig. 2. A).

To further explore the characteristics of neutrophil differentiation from CD371$^+$ GMPs, we first analyzed CD115$^+$ progenitor proportions at different time points, and subsequently analyzed the neutrophil differentiation potential from CD115$^+$-excluded progenitor cells. The percentages of CD115$^+$ cells increased up to 75% on day 5, and the neutrophil purity increased to 80% (Fig. 2. G). Thus, we postulated that neutrophil commitment could be stimulated by gradual loss of monocyte differentiation potential (Fig. 2. H). To test this hypothesis, we measured a set of surface markers in CD371$^+$ CD115$^-$ CD66b$^-$ CD14$^-$ cells on day 14 to further improve neutrophil purity. CD371$^+$ CD115$^-$ CD66b$^-$ CD14$^-$cells expressed CD1c, CD73, and CD116, while CD371$^+$ CD66b$^+$ neutrophils did not express these markers (Supplementary Fig. 2. B). In addition, we also analyzed *in vitro* early differentiation of GMPs at day 5 and *in vivo* CD34$^+$ HSPCs transplanted NSG-BM. Both *in vitro* and *in vivo* studies demonstrated that CD123$^+$CD371$^+$CD115$^-$CD66b$^-$ cells contained CD116/CD1c/CD73 positive cells (Supplementary Fig. 2. C). Excluding CD116/CD1c/CD73 positive cells from the CD115$^-$ progenitors could improve neutrophil purity.

Subsequently, we sorted CD34^{mid} CD371$^+$, CD34^{low} CD371$^+$ and CD66b$^-$ CD371$^+$, CD66b$^+$ CD371$^+$ cells (Fig. 2. I) within the CD115/CD116/CD73/CD1c$^-$ CD123^{mid} CD38$^+$ population derived from CD371$^+$ CD115$^-$ GMPs. CD34^{mid} CD371$^+$ progenitors gave rise to approximately 80% neutrophils, while CD34$^-$ CD371$^+$ CD66b$^-$ late-committed neutrophil progenitors produced more than 90% neutrophils (Fig. 2. J). In addition, we also sorted equal populations from CB-transplanted B-NDG-SM (expressing human SCF and GM-CSF) BM (Fig. 2. K). In a 6–9 days culture of the sorted populations, we found that CD34^{low} CD371$^+$ and CD34$^-$ CD371$^+$ cells produced CD15$^+$ CD66b$^+$ neutrophils of high purity (Fig. 2 L). Conclusively, we preliminary validated the differentiation model of neutrophils, in which CD371$^+$ CD115$^-$ GMPs gradually lose monocyte differentiation potential to become neutrophil progenitors (Fig. 2. H).

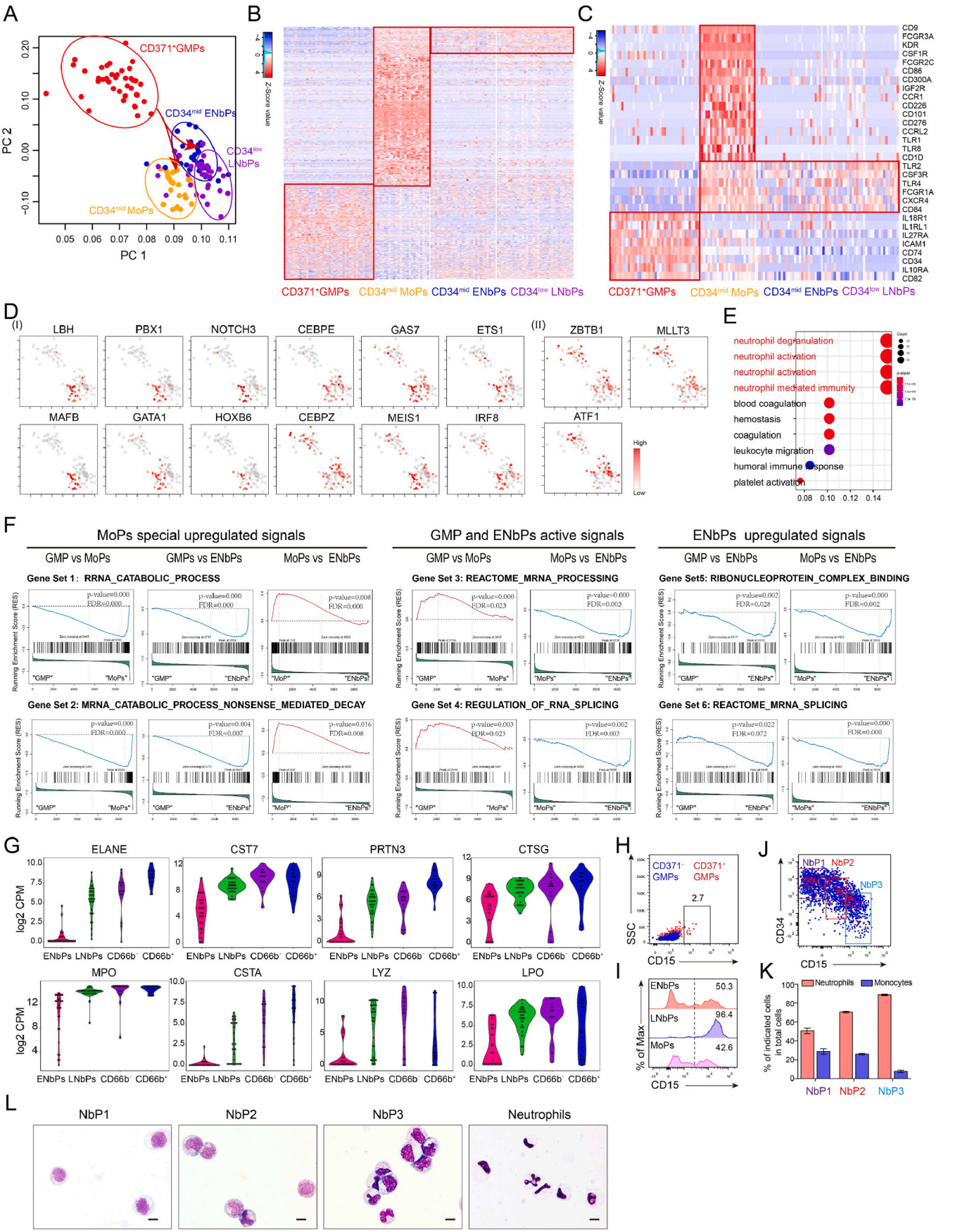

(caption on next page)

Fig. 3. Dissecting the transcriptome characterization of neutrophil differentiation from CD115$^-$CD371$^+$ GMPs at the single-cell level.
(A) Principal component analysis (PCA) of CD115$^-$ CD371$^+$ GMPs, CD115$^-$ CD371$^+$ GMP-derived CD34^{mid} ENbPs, CD34^{low} LNbPs and CD34^{mid} CD115$^+$ MoPs. The CPM (count per million) values of genes expressed by CD115$^-$ CD371$^+$ GMPs (n = 40), CD34^{low} ENbPs (n = 29), CD34^{low} LNbPs (n = 34) and CD34$^+$ CD115$^+$ MoPs (n = 24) were calculated by pcaMethod packages.
(B) Heatmaps showing the expression pattern of different populations by all DEGs (p-value < 0.01, log2 fold change >2).
(C) Heatmaps representing the differential expression of surface markers in CD371$^+$ CD115$^-$GMPs, MoPs, ENbPs and LNbPs.
(D) Density plots presenting the expression levels of representative differentially expressed transcription factors.
(E) GO enrichment analysis of genes upregulated in CD34^{mid} neutrophil-biased progenitors relative to CD371$^+$ GMPs.
(F) GSEA analysis of the active signals in CD371$^+$ CD115$^-$GMPs (GMP), MoPs, and ENbPs.
(G) Violin plots indicating the expression levels of granule generation-related genes in neutrophil-biased progenitors and neutrophil progenitors.
(H–I) Representative flow cytometry plots of CD15 expression on CD371$^-$ CD115$^-$ GMPs, CD371$^+$ CD115$^-$ GMPs, Lin$^-$ CD116$^-$ CD1c$^-$ CD73$^-$ CD115$^-$ CD123^{mid} CD371$^+$ CD34^{mid} ENbPs, Lin$^-$ CD116$^-$ CD1c$^-$ CD73$^-$ CD115$^-$ CD123^{mid} CD371$^+$ CD34^{low} LNbPs and CD115$^+$ CD34^{mid} MoPs derived from CD371$^+$ GMP cultures. The numbers indicate the percentages.
(J–K) Neutrophil differentiation potentials of CD34$^+$ CD15$^-$ (NbP1), CD34^{mid} CD15^{mid} (NbP2), and CD34$^{low/-}$CD15$^+$ (NbP3) sorted from Lin/CD116/CD1c/CD73$^-$ CD115$^-$ CD123^{mid} CD371$^+$ cells at day 3 of CD371$^+$ CD115$^-$ GMP culture.
(L) MGG staining assays indicating the morphologies of defined NbP1s, NbP2s, NbP3s, and neutrophils. Scale bar = 10 μm. Data in **(K)** are represented as means ± SD.

3.3. Single-cell transcriptome reveals the characteristics of neutrophil commitment

To reveal the commitment characteristics of neutrophil progenitors from a transcriptome perspective, we performed single-cell RNA-seq to evaluate transcriptomic changes. We sorted CD371$^+$ CD34$^+$ CD115$^-$ GMPs, CD115$^-$ CD34^{mid} CD371$^+$ early neutrophil biased progenitors (ENbPs), CD115$^-$ CD34^{low} CD371$^+$ late neutrophil biased progenitors (LNbPs), and CD34^{mid} CD115$^+$ monocyte progenitors (MoPs) (Fig. 2. I, Supplementary Fig. 3. A) to generate dsDNA from mRNA as previously reported [28], and constructed libraries for sequencing with 1 ng dsDNA [21,33]. We performed principal component analysis to determine the relationship of CD34^{mid} CD115$^+$ MoPs, CD34^{low} CD371$^+$ ENbPs, CD34$^-$ CD371$^+$ LNbPs, and CD371$^+$ CD115$^-$ GMPs (Fig. 3. A). First, we analyzed the expression pattern of previously reported neutrophil progenitor high expression markers [4]. The high expression surface markers were expressed in ENbPs, LNbPs and MoPs (Supplementary Fig. 3. B). Differential expression genes (DEGs) ($p < 0.01$, log2foldchange >2) analysis was performed to screen out genes uniquely expressed in neutrophils. Only a set of upregulated genes was uniquely expressed in MoPs, but not in ENbPs or LNbPs compared with CD371$^+$ CD115$^-$ GMPs (Fig. 3. B).

To further identify the characteristics of neutrophil commitment, we analyzed the expression pattern of neutrophil surface markers and transcription factors. Differentially expressed surface markers revealed that in CD115$^+$CD34^{mid} MoPs, the surface markers CD9, KDR, IGF2R, TLR8, CD1d, CD86, CD300A, FCGR3A(CD16) were specifically upregulated, and that FCGR1A(CD64). CSF3R, TLR2, TLR4, CXCR4, and CD84 were moderately expressed in ENbPs and LNbPs (Fig. 3. C). Furthermore, we screened out differentially ($p < 0.01$, log2foldchange >2) expressed transcription factors, revealing that the monocyte- or dendritic cell-related transcription factors MAFB [34,35], MAF [36], PBX1, HOXB6 [37], IRF8 [38,39] were upregulated in MoPs (Fig. 3. D. (I)), while the reported mice neutrophil master regulator factor CEBPE [40] was expressed in both MoPs and neutrophil progenitors (Fig. 3. D. (I)). Unexpectedly, only three transcription factors, ZBTB1, ATF1, and MLLT3, were differentially expressed in ENbPs and LNbPs (Fig. 3. D. (II)). However, gene ontology (GO) enrichment analysis of genes upregulated in ENbPs ($p < 0.01$, log2foldchange >2) relative to those in CD371$^+$ CD115$^-$ GMPs indicated that neutrophil degranulation, neutrophil activation, and neutrophil-mediated immunity genes were upregulated in neutrophil-biased progenitors (Fig. 3. E). To analyze the signals altered by differentiation of CD371$^+$ CD115$^-$ GMPs into MoPs and ENbPs, we performed gene set enrichment analysis (GSEA). rRNA catabolic processing-, rRNA binding-, and mRNA decay-related signals were upregulated in both MoPs and ENbPs, with more robust signal changes in MoPs relative to ENbPs. In addition, both CD371$^+$ CD115$^-$ GMP and ENbPs highly expressed genes related to RNA splicing signaling pathways, while ENbPs had stronger mRNA splicing signals (Fig. 3. F, Supplementary Fig. 3. C).

Additionally, we sorted CD116$^-$ CD1c$^-$ CD115$^-$ CD123$^+$ CD34$^-$ CD66b$^-$ CD371$^+$ and CD66b$^+$ CD371$^+$ cells (Supplementary Fig. 3. A) from cultures of CD371$^+$ CD115$^-$ GMPs at day 7 for single-cell RNA-seq. Among the four populations, only 75 DEGs were identified. Among DEGs, only granule-related genes and genes highly expressed in neutrophils, including LPO, MPO, LYZ [41], ELANE, PRTN3, CSTG [42], CST7 [43], and CSTA were upregulated by differentiation into neutrophils (Fig. 3. G). Taken together, these findings indicated that neutrophil-biased progenitors had a similar transcriptome pattern, suggesting that the further differentiation of neutrophil-biased progenitor cells into committed neutrophil progenitor cells could be regulated by post-transcriptional modifications.

To further identify the specific surface markers for MoPs and neutrophil-biased progenitors, we used flow cytometry to analyze the surface expression of CD15, FCGR1A (CD64), TLR2, TLR4, CXCR4, and CSF3R (CD114), which were upregulated in MoPs, ENbPs, and LNbPs relative to CD371$^+$ CD115$^-$ GMPs (Fig. 3. C). Although both CD64 and CD15 were significantly upregulated in ENbP to LNbP (Supplementary Fig. 3. D), CD64 was expressed in both monocytes and neutrophils [44] and moderately expressed in neutrophil committed progenitors [6], so we further analyzed the expression of CD15 in the process of CD371$^+$CD115$^-$ GMPs to LNbPs. Surprisingly, CD15 was first expressed at low levels in CD371$^+$ CD115$^-$ GMPs, and highly expressed in LNbPs (Fig. 3 H-I). Thus, we postulated that the expression level of CD15 could be indicative of the neutrophil differentiation potential of neutrophil-biased progenitors. Sequentially, we sorted CD34$^+$ CD15$^-$ (NbP1), CD34^{mid} CD15^{mid} (NbP2), and CD34$^{low/-}$ CD15$^+$ (NbP3) cells gated from CD1c/CD73/CD116$^-$ CD115$^-$CD123$^+$CD371$^+$ cells derived from CD371$^+$ GMP cultures at day 3 to analyze the neutrophil differentiation potential. The neutrophil differentiation potential was enhanced, together with increased expression of CD15 and decreased expression of CD34 (Fig. 3 J-K). A morphology assay of the different stages of neutrophil differentiation also indicated a gradual change in cell morphology (Fig. 3 L). Together, these findings indicated that CD15 expression is specific to the neutrophil differentiation potential of neutrophil-biased progenitors.

3.4. Dissecting the characteristics of the human neutrophil lineage commitment process in adult bone marrow at the single-cell level

To further validate the commitment characteristics of neutrophil-biased progenitors in adult human BM, we analyzed the expression pattern of CD34 and CD15 gated from Lin/CD1c/CD116/CD73/CD115$^-$ CD371$^+$ CD123$^+$ CD45RA$^+$ cells by flow cytometry. The same expression pattern of CD34 and CD15 was observed in human adult BM as in the *in vitro* model (Fig. 4. A). In addition, neutrophil and monocyte

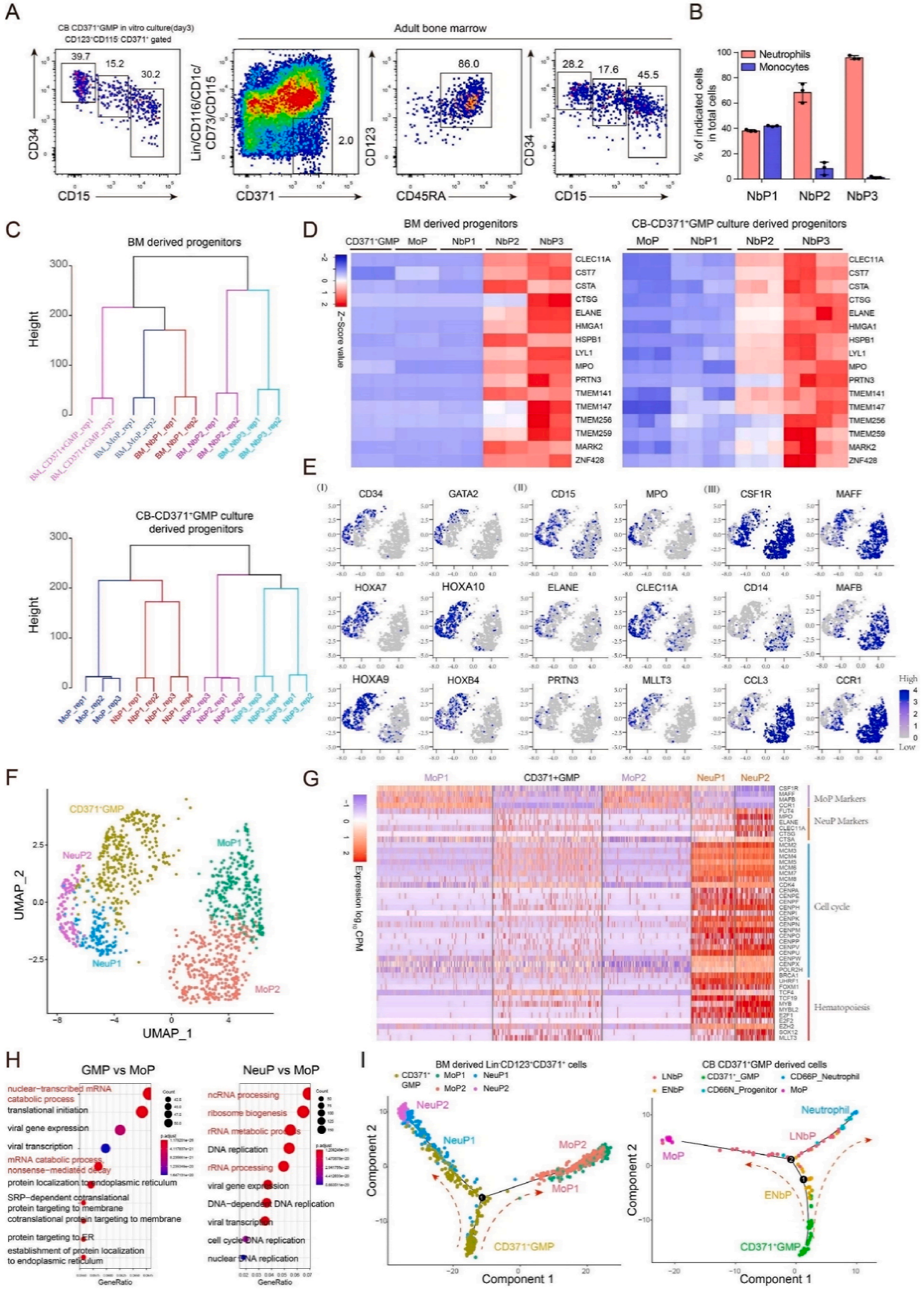

(caption on next page)

Fig. 4. Characteristics of neutrophil differentiation in human bone marrow at the single-cell level.
(A) Representative flow cytometry plots of neutrophil-biased progenitors in adult human BM.
(B) Neutrophil differentiation potential analyses of $CD34^{+}$ $CD15^{-}$ NbP1, $CD34^{mid}$ $CD15^{mid}$ NbP2s and $CD34^{low/-}$ $CD15^{+}$ NbP3s sorted from adult human BM Lin/CD116/CD1c/$CD73^{-}$ $CD115^{-}$ $CD371^{+}$ $CD123^{mid}$ $CD45RA^{+}$ cells. Flow cytometry assay to performed to analyze the $CD11b^{+}CD15^{+}CD66b^{+}CD14^{-}$ neutrophils and $CD11b^{+}$ $CD66b^{-}CD14^{+}$ monocytes in total cells at day 6 to day 10.
(C) Unsupervised cluster analysis of bulk cell RNA-seq data from neutrophil-biased progenitors and monocyte progenitors derived from adult human BM and cultures of CB $CD371^{+}$ GMPs at day 3.
(D) Heat maps showing representative highly expressed genes in neutrophil-biased progenitors.
(E–F) UMAP analysis of representative highly expressed genes in $CD371^{+}$ GMPs, neutrophil related progenitors (NeuP1 and NeuP2), MoP related progenitors (MoP1, and MoP2).
(G) Heatmaps presenting highly expressed genes in adult human bone marrow-derived neutrophil related progenitors (NeuP1 and NeuP2).
(H) GO enrichment analysis of DEGs in CD371+ GMPs compared to MoPs and NeuPs compared to MoPs.
(I) Single-cell trajectory analysis of neutrophil progenitors and monocyte progenitors derived from human adult BM $CD371^{+}$ GMP, NeuP1, NeuP2, MoP1, MoP2 and MoP, NbP1, NbP2, NbP3, $CD66b^{+}$ neutrophils derived from CB $CD115^{-}$ $CD371^{+}$ GMPs. Data in **(B)** are represented as the means ± SD.

differentiation potential assays of $CD34^{+}$ $CD15^{-}$ NbP1, $CD34^{mid}$ $CD15^{mid}$ NbP2 and $CD34^{low/-}$ $CD15^{+}$ NbP3 cells indicated that human neutrophil progenitors also committed gradually with decreased CD34 and increased CD15 expression (Fig. 4. B), which was consistent with the *in vitro* results (Fig. 3. K).

Unsupervised cluster analysis of bulk cell RNA-seq data of MoPs and neutrophil-biased progenitors both *in vivo* and *in vitro* indicated that neutrophil-biased progenitors had similar transcriptomic characteristics to those of MoPs (Fig. 4. C). We performed DEG analysis to screen a list of genes that are highly expressed in neutrophil-biased progenitors (Supplementary Fig. 4. A). We found that both *in vivo*- and *in vitro*-derived neutrophil-biased progenitors highly expressed neutrophil uni-expressed genes or granule-related genes, including MPO, LRG1 [45], PRTN3, ELANE, CTSG [42], CST7 [43], CSTA [46], and CLEC11A [47] (Fig. 4. D).

To further delineate the neutrophil commitment characteristics in adult human BM, we performed single-cell RNA-seq of sorted Lin/CD116/CD1C/$CD73^{-}$ $CD123^{+}$ $CD371^{+}$ populations (Supplementary Fig. 4. B) that contained neutrophil-biased progenitors at different stages of differentiation. The Seurat R software package was used for cluster identification (Supplementary figure 4 C-D). We first excluded populations of dendritic progenitor cells that highly expressed CD1c, CCR6 [48], CLEC10A [49], CD1E [50], CLECL1 [51], GZMB [52] (Supplementary Fig. 4. E). Subsequently, GATA2, HOXA9, HOXA10, HOXB4, MPO, PRTN3, ELANE, CLEC11A, MAFB, CD115, and CD14 were used to identify early $CD371^{+}$ GMPs, neutrophil related progenitors named NeuP1 and NeuP2 (not equal to the NbP1, NbP2 and NbP3 defined by CD34 and CD15 at protein level), and monocyte progenitors named MoP1 and MoP2 (not equal to $CD34^{mid}$ $CD115^{+}$MoPs). $CD371^{+}$ GMPs exhibited high expression of the transcription factors GATA2, HOXA9, HOXA10, HOXB4, and HOXA7, and neutrophil related progenitors (NeuP1, NeuP2) exhibited high expression of CD15 (FUT4), PRTN3, MPO, ELANE, MLLT3, and CLEC11A. Monocyte progenitors highly expressed MAFF, MAFB, CD115 (CSF1R), CD14, CCL3, and CCR1 (Fig. 4 E-F). Further, monocyte progenitors also expressed surface markers that were highly expressed in MoPs *in vitro*, including TLR2, TLR4, IGF2R, FCGR2A, FCGR2B, CCR1, CD226, CD267, and CD86 (Supplementary Fig. 4. F, Fig. 3. C). Furthermore, neutrophil-related progenitors highly expressed DNA replication- and myeloid differentiation-related transcription factors, including TCF4, which is related to granulopoiesis [53] (Fig. 4. G, Supplementary Fig. 4. G). In addition, GO enrichment analysis revealed that DEGs in $CD371^{+}$ $CD115^{-}$ GMP cells compared to MoPs and NeuPs compared to MoPs were also mainly related to mRNA processing and rRNA processing (Fig. 4. H), which was similar to *in vitro* signal changes (Fig. 3. F). Finally, a single-cell trajectory assay was performed to evaluate the relationship between $CD371^{+}$ $CD115^{-}$ GMPs, neutrophil-related progenitors, and monocyte progenitors. Both *in vivo* and *in vitro*-derived cells shared a similar cell trajectory, and neutrophil progenitors were more similar to $CD371^{+}$ $CD115^{-}$ GMPs (Fig. 4. I). Together, these results indicated that the transcriptomes of $CD371^{+}$ $CD115^{-}$ GMPs, neutrophil-related progenitors, and monocyte progenitors had similar developmental characteristics both *in vivo* and *in vitro*.

3.5. ALA targets ELK1 to regulate neutrophil differentiation

To further identify the key regulatory genes of neutrophil differentiation, we analyzed the effects of ALA on neutrophil differentiation of neutrophil-biased progenitor cells ($CD34^{+}$ $CD15^{-}$ NbP1, $CD34^{mid}$ $CD15^{mid}$ NbP2, $CD34^{low/-}$ $CD15^{+}$ NbP3) (Supplementary Fig. 5. A) derived from $CD371^{+}$ $CD115^{-}$ GMPs at day 3. ALA significantly impeded neutrophil differentiation from NbP1, NbP2, and NbP3 cells, with the most potent blockage of NbP1 cells giving rise to neutrophils (Fig. 5. A). Based on this model, we performed bulk cell RNA-seq to analyze the transcriptomic changes of NbP1 and NbP2 cells ± ALA. Downregulated DEGs were 5-fold greater than upregulated DEGs (Fig. 5. B). The downregulated genes were more related to neutrophil activity (Fig. 5. B). About 120 neutrophil-specific genes were downregulated by ALA, including PRTN3 [54], LRG1 [45], CEBPE [55], LPO, MPO, ELANE [6, 56], CLEC11A [57] and KLF16, CTS7, HMGA1 (Fig. 5. C, Supplementary Fig. 5. B).

To identify the primary neutrophil commitment regulatory genes, we first cloned cDNAs of CEBPE, LRG1, PRTN3 and CLEC11A into PCCL-desRed or PCCL-EGFP overexpression vectors [27], and the shRNA target sequences of these genes into plKO.1-GFP vectors. Both over-expression and shRNA knockdown experiments indicated that CEBPE, PRTN3, LRG1, and CLEC11A did not affect human neutrophil differentiation (Supplementary Fig. 5. C). Given that granule-related genes MPO, ELANE, PRTN3, LRG1, and CLEC11A do not affect neutrophil differentiation, we analyzed ALA-downregulated transcription factors in NbP1 and NbP2 cells. We identified 38 differentially expressed (p.adj, $<$ 0.05; foldchange, $>$ 1.5) transcription factors (Fig. 5. D). GO enrichment analysis demonstrated that these transcription factors were related to epigenetic remodeling events such as chromosome organization, chromatin remodeling, and heterochromatin assembly (Supplementary Fig. 5. D), including ELK1 reported to interact with CSF-1R (CD115) [58]and regulate micro-RNA expression in monocyte differentiation [59]. To determine the function of these transcription factors in neutrophil differentiation, overexpression of XRCC3, TMEM176B, PBX3, MDM1, MDB3, HMGA1 and knockdown of B3GAT3, ELK1, E2F1, HSF1, KLF16, MLLT1, MYBL2, SNRPB, SSBP4, TRIM28, and ZDHHC13 in $CD34^{+}$ HSPCs was performed to analyze neutrophil differentiation potential. Overexpression of XRCC3, TMEM176B, PBX3, MDM1, MDB3, HMGA1 (Supplementary Fig. 5. E) and knocking down of B3GAT3, E2F1, HSF1, KLF16, MLLT1, MYBL2, SNRPB, SSBP4, TRIM28, and ZDHHC13 did not affect neutrophil differentiation (Fig. 5. E), while ELK1 knocking down significantly impeded neutrophil differentiation and promoted monocyte differentiation (Fig. 5 E-F). Additionally, ALA downregulated ELK1 expression at the protein level, as demonstrated by immunofluorescence analysis (Fig. 5. G).

To reveal the roles of ELK1 in early neutrophil progenitor commitment, we analyzed the neutrophil differentiation potential of ELK1-

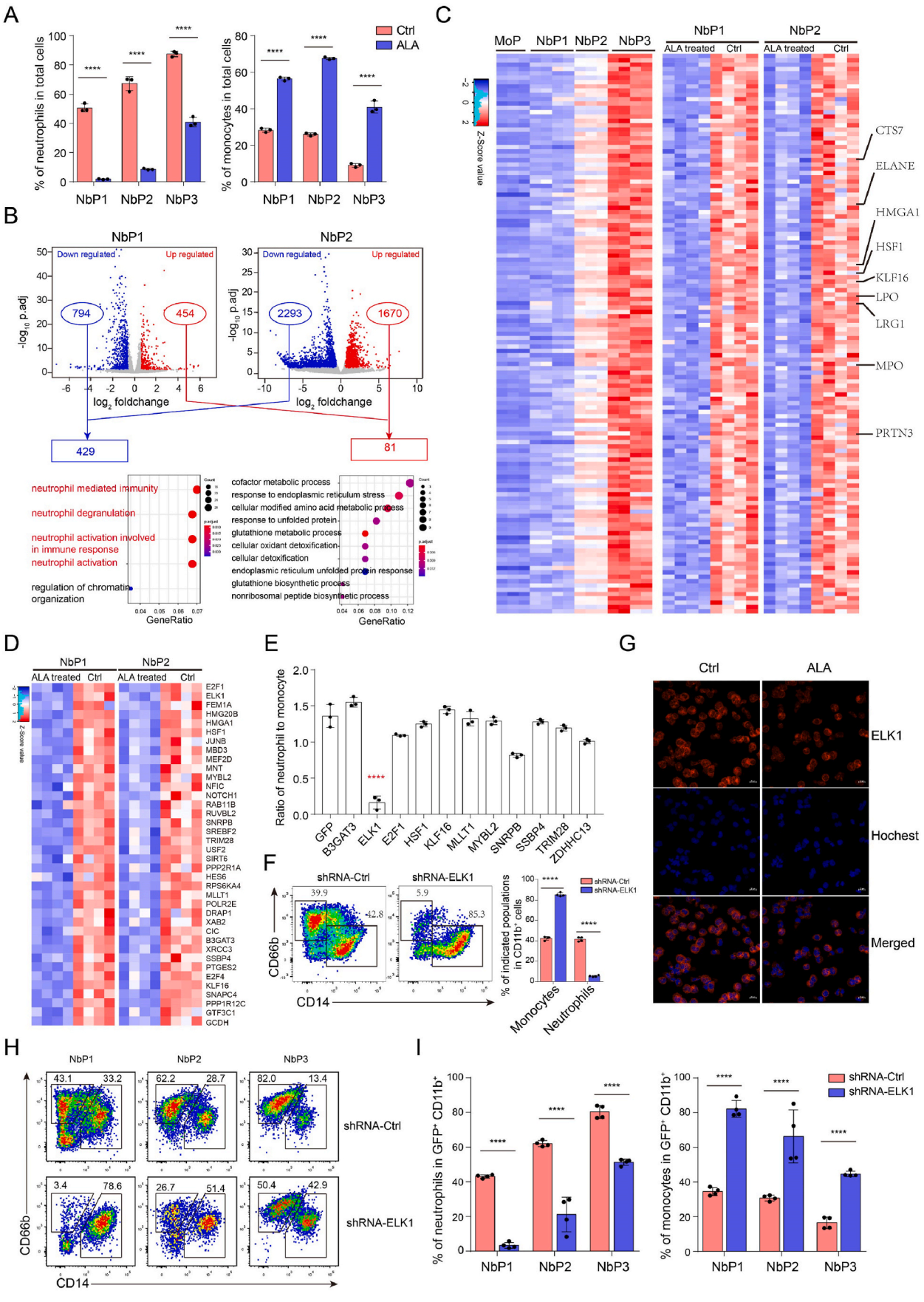

(caption on next page)

Fig. 5. ALA regulates commitment of neutrophil progenitors by targeting ELK1.
(A) Statistical analysis of neutrophils and monocytes differentiated from NbP1s, NbP2s, and NbP3s ± ALA treatment. To analyze the effect of ALA on neutrophil differentiation, sorted neutrophil biased progenitors were cultured ± ALA and flow cytometry assay to performed to analyze the $CD11b^+CD15^+CD66b^+CD14^-$ neutrophils and $CD11b^+$ $CD66b^-CD14^+$ monocytes at day6 to day14.
(B) Volcano plots and GO enrichment analysis of genes upregulated and downregulated by ALA.
(C) Heatmaps showing ALA-downregulated genes among neutrophil-biased progenitor-specific genes.
(D) Heatmaps presenting ALA-downregulated transcription factors in NbP1s and NbP2s.
(E) Flow cytometry analysis of neutrophils and monocytes derived from $CD34^+$ HSPCs transduced with shRNAs targeting ALA-downregulated transcription factors. The ratio of neutrophils to monocytes is presented to analyze the neutrophil differentiation potential of $CD34^+$ HSPCs transduced with different shRNAs.
(F) Flow cytometry plots of neutrophils and monocytes from ELK1-shRNA knockdown $CD34^+$ progenitors. Flow cytometry analysis was performed on day 9, and neutrophils and monocytes were analyzed with $CD11b^+$ gated cells. Representative flow cytometry plots and statistical analysis bar plots are shown.
(G) Immunofluorescence analysis of ELK1 was performed to measure ELK1 protein levels in NbP1 cells ± ALA treatment. Scale bar = 20 μm.
(H–I) *In vitro* flow cytometry analysis of neutrophils and monocytes from ELK1-shRNA-transduced NbP1, NbP2, and NbP3 cells. Flow cytometry analysis was performed from day 6 to day 9, and neutrophils and monocytes were analyzed within GFP^+ $CD11b^+$ gated cells. Representative flow cytometry plots **(G)** and statistical analysis bar plots **(H)** are shown.
Data in **(A, E, I)** are expressed as means ± SD. An unpaired Student's *t*-test (two-tailed) was performed to assess statistical significance. NS = not significant, *P < 0.05, **P < 0.01, ***P < 0.001, ****P < 0.0001, N = 3–4.

shRNA transduced NbP1, NbP2, and NbP3 cells. Knocking down ELK1 had the same effect as ALA on the commitment of neutrophil progenitors (Fig. 5. A, H–I). Taken together, these findings indicated that ALA impeded neutrophil differentiation by targeting ELK1, and that ELK1 was required for granulopoiesis.

3.6. SF3B1 regulates ELK1 RNA splicing

Because ELK1 is essential for human neutrophil differentiation, we overexpressed ELK1 in $CD34^+$ HSPCs to increase neutrophil differentiation. Unexpectedly, overexpression of the ELK1 long coding protein isoform (L-ELK1) also impeded neutrophil differentiation (Fig. 6. A). Thus, we hypothesized that different ELK1 isoforms could play different roles in balancing neutrophil and monocyte differentiation. PCR analysis of ELK1 isoforms indicated that $CD34^{mid}$ MoPs highly expressed theL-ELK1, while neutrophil-biased progenitors highly expressed the short coding protein isoform (S-ELK1) (Fig. 6. B). Furthermore, immunofluorescence staining for L-ELK1 indicated by the ELK1 C- terminus antibody and S-ELK1 (absent the C- terminus domain) indicated by ELK1 N- terminus antibody (measure both L-ELK1 and S-ELK1) deduct C-terminus antibody (measure L-ELK1 only) showed that monocyte progenitors and monocytes highly expressed L-ELK1, while neutrophil progenitors and neutrophils highly expressed S-ELK1 (Fig. 6. C). Further analysis demonstrated that ALA downregulated the expression of S-ELK1 but not L-ELK1 (Supplementary Fig. 6. A).

Because single-cell transcriptome findings demonstrated that ENbPs had stronger RNA splicing signals (Fig. 3. E), we further analyzed the changes in ELK1 RNA splicing ± ALA. The results indicated that ALA significantly changed RNA splicing and spliceosome-related signals (Fig. 6. D). DEG analysis revealed that ALA-upregulated splicing factors such as SRSF3, SRSF11, SF3B1, and downregulated SF3B4 and SF3B5, which were differentially expressed in MoPs and neutrophil-biased progenitors (Fig. 6. E, Supplementary Fig. 6. B). Furthermore, mass spectrometry analysis of ELK1 RNA pull-down proteins demonstrated that most of the pulled-down proteins were related to RNA splicing and RNA binding (Fig. 6 F-G). Further, the ALA-upregulated splicing factors SF3B1 and SRSF1 accounted for a high proportion of the identified ELK RNA-binding proteins (Fig. 6. H). Thus, we determined the functions of SRSF1 and SF3B1 in neutrophil differentiation. SF3B1 knockdown significantly increased the production of neutrophils and decreased monocyte percentages (Fig. 6. I, Supplementary Fig. 6. C).

We postulated that ELK1 isoform expression could be controlled by SF3B1. We analyzed the RNA-protein interaction of ELK1 RNA and SF3B1 ± ALA. These findings demonstrated that SF3B1 bound the splicing site of ELK1 mRNA, and that treatment with ALA increased the binding of SF3B1 to ELK1 mRNA (Fig. 6. J). In addition, SF3B1 knockdown partially impaired the effects of ALA on neutrophil and monocyte differentiation (Supplementary figure 6 C-D). Immunofluorescence also indicated that SF3B1 downregulated L-ELK1 and upregulated S-ELK1 (Fig. 6. K). Taken together, these findings demonstrated that SF3B1 regulated neutrophil and monocyte differentiation from $CD371^+$ $CD115^-$ GMPs by regulating expression of S-ELK1 and L-ELK1.

3.7. L-ELK1 and S-ELK1 have differential roles in human neutrophil differentiation

To analyze the effects of L-ELK1 and S-ELK1 on neutrophil and monocyte differentiation derived from $CD34^+$ HSPCs, we sorted Ctrl (GFP control virus), L-ELK1, S-ELK1 and ELK1-shRNA-A and ELK1-shRNA-L transduced $CD34^+$ HSPCs to perform *in vitro* differentiation culture or transplant into NDG-SM mice. Both *in vivo* and *in vitro* data demonstrated that L-ELK1 overexpression impaired neutrophil differentiation, while knockdown of only L-ELK1 enhanced neutrophil differentiation (Supplementary figure 7 A-B). However, flow cytometric analysis of NbP1 cells overexpressing of L-ELK1 and S-ELK1 or knocking down of ELK1 demonstrated that L-ELK1 inhibited $CD15^+CD66b^+$ expression but did not block expression of $CD11b^-$ $CD14^-$ $CD66b^-$ $CD15^+$, a characteristic of NbP1s (Fig. 7. A). Thus, we postulated that L-ELK1 was required for early commitment of neutrophil progenitors (NbP1, NbP2, and NbP3), but not for committed neutrophil progenitors ($CD15^+$ $CD66b^+$). Giemsa staining also revealed that overexpression of L-ELK1 suppressed most of the cells at the $CD115^-$ $CD34^-$ $CD11b^-$ $CD15^+$ NbP3 stage (Fig. 7. B). Subsequently, we sorted $CD115^-$ $CD34^+$ $CD371^+$ $CD15^-$ NbP1s from L-ELK1-OE-, S-ELK1-OE-, and ELK1-shRNA-A-transduced progenitors at day 3 for further differentiation analyses. Both L-ELK1 and S-ELK1 overexpression upregulated CD15, while ELK1 knockdown downregulated CD15 at an early stage (Fig. 7. C). Overexpression of L-ELK1 or knockdown of ELK1 significantly decreased CD66b expression. In addition, overexpression of L-ELK1 and S-ELK1 did not block $CD14^+$ monocyte differentiation, while ELK1 knockdown enhanced monocyte differentiation (Fig. 7. C). This indicated that L-ELK1 was required for early neutrophil progenitor commitment and was gradually downregulated with commitment.

To further identify the key signals altered by L-ELK1 or S-ELK1 in neutrophil differentiation, we performed RNA-seq analysis of L-ELK1- and S-ELK1-transduced $CD34^+$ $CD371^+$ $CD115^-$ $CD123^+$ $CD38^+$ progenitors ($CD371^+$ $CD115^-$ GMPs). DEG (Fig. 7. D) (p.adj, < 0.05; log2 fold change, > 1) analysis revealed that over 75% of DEGs were upregulated or downregulated in both L-ELK1- and S-ELK1-transduced $CD371^+$ $CD115^-$ GMPs (Supplementary Fig. 7. C). Because L-ELK1 and S-ELK1 have differential roles in regulating neutrophil or monocyte differentiation, we further analyzed DEGs in L-ELK1, S-ELK1 or Ctrl cells (Fig. 7. E). Surprisingly, GO enrichment analysis revealed that genes specifically upregulated by L-ELK1 were significantly enriched for neutrophil activation, neutrophil-mediated immunity, and neutrophil degranulation (Fig. 7. F). This trend was not observed for S-ELK1 DEGs.

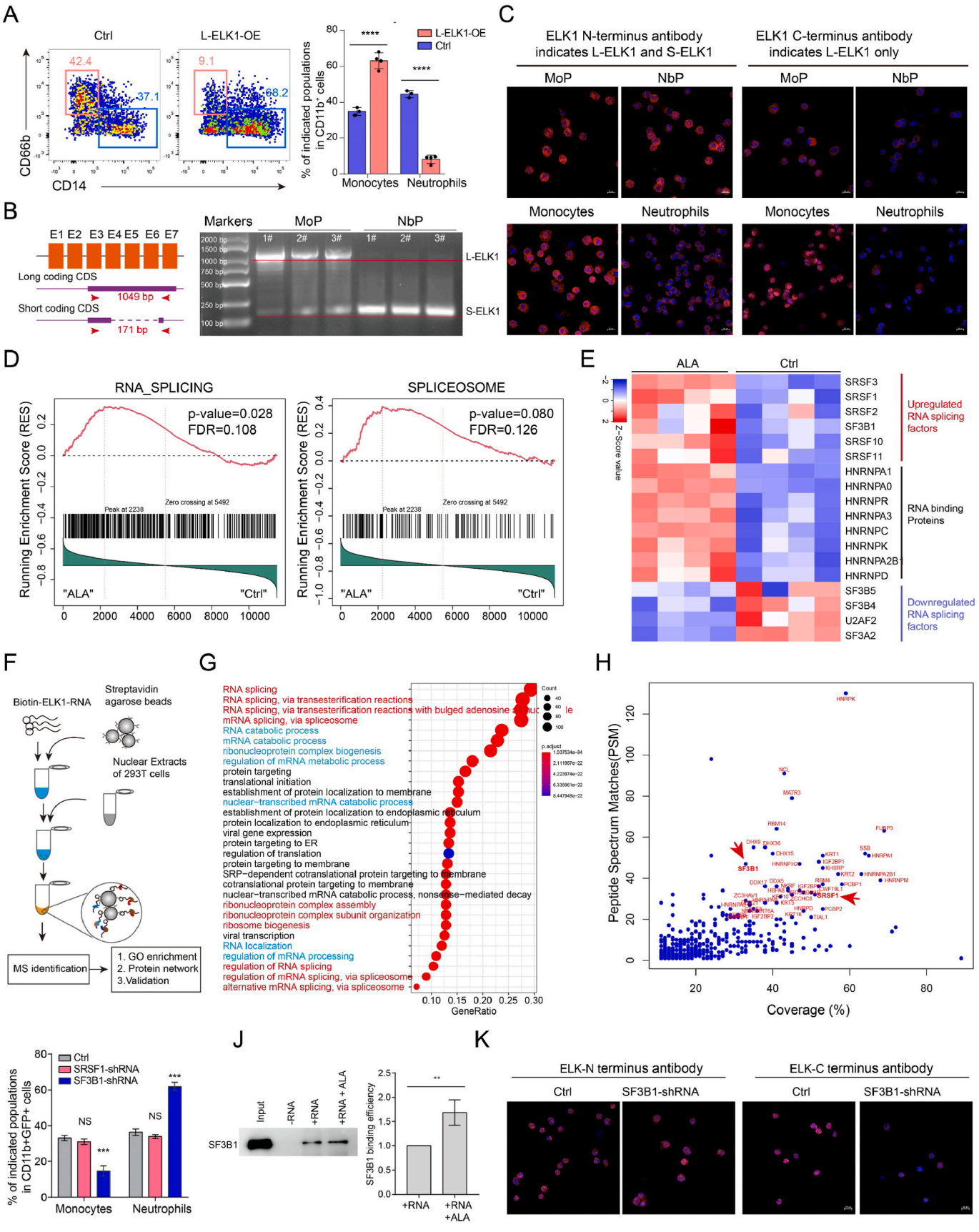

(caption on next page)

Fig. 6. SF3B1 regulates ELK1 mRNA splicing.
(A) Flow cytometry analysis of neutrophils and monocytes derived from L-ELK1-overexpressing $CD115^{-}$ $CD34^{+}$ progenitors. Flow cytometry analysis was performed on day 9.
(B). Identification of different ELK1 isoforms in MoPs and NbPs by PCR. Ten nanograms of dsDNA generated from MoPs or neutrophil-biased progenitors (NbPs) was used for PCR.
(C) Immunofluorescence for ELK1 N-terminus and ELK1 C terminus antibodies were performed to assess L-ELK1 and S-ELK1 expression levels in MoPs and neutrophil biased progenitor (NbP2, NbP3) cells. For the absence of C-terminus domain of S-ELK1, the C-terminus antibody indicates L-ELK1 only and the ELK1 N-terminus antibody indicates both L-ELK1 and S-ELK1.
(D) GSEA was performed to analyze the effect of ALA on RNA splicing-related signal changes in NbP1.
(E) Heatmaps present ALA-upregulated and ALA-downregulated RNA splicing-related genes.
(F) Flow diagram for mass spectrometry (MS) analysis of ELK1 RNA pull-down proteins.
(G) GO enrichment analysis of ELK1 RNA pull-down proteins. Proteins with coverage >10% (391 proteins) were subjected to GO enrichment analysis.
(H) Scatter plots showing the relationship of peptide-spectral matches (PSM) and protein coverage. Proteins with coverage >30% and PSM >20 are denoted by red gene names.
(I) Statistical analysis of the proportions of neutrophils and monocytes derived from SRSF1 shRNA- and SF3B1 shRNA-transduced $CD371^{+}$ $CD115^{-}$ GMPs. Flow cytometry analysis was performed on day 14 of differentiation.
(J) RNA pull-down and immunoblotting were performed to measure the interaction of ELK1 RNA and SF3B1 under ALA treatment.
(K) Immunofluorescence staining for ELK1 N-terminus and ELK1 C- terminus antibodies were performed to assess L-ELK1 and S-ELK1 expression levels in SF3B1-shRNA transduced NbP1 cells and Ctrl NbP1 cells. For the absence of C-terminus domain of S-ELK1, the C- terminus antibody indicates L-ELK1 only and the ELK1 N-terminus antibody indicates L-ELK1 and S-ELK1 Data in **(A, I)** are represented as the means ± SD. An unpaired Student's *t*-test (two-tailed) was performed to determine statistical significance. NS = not significant, *P < 0.05, **P < 0.01, ***P < 0.001, ****P < 0.0001, N = 3–7. **(C, J)** Scale bar = 20 μm. (For interpretation of the references to color in this figure legend, the reader is referred to the Web version of this article.)

GO function classification revealed that S-ELK1 upregulated catalytic activity-related genes and downregulated transporter activity-related genes (Fig. 7. G). GSEA also demonstrated that S-ELK1 significantly changed genes related to catalytic processing, ligase activity, and ER-to-Golgi transport (Fig. 7. H). Further DEG analysis revealed that L-ELK1 increased genes related to enzyme synthesis (CTSS, CTSB, CSTB, HEXB, FUCA1 PRCP, etc.) and endoplasmic reticulum to Golgi transport (COPA, COG6, GOLGB1, BET1, LMAN1, USO1, VAPA, BET1, etc.), while S-ELK1 upregulated additional genes related to endoplasmic reticulum to Golgi transport (SEC24A, SEC23IP and KIF3A), catalytic reactions, and enzyme maturation-related genes (LTN1, TRIM37, TRIM71, and LOXL1) (Fig. 7. I).

In summary, the expression of the surface marker CD15 can be used to define the degree of neutrophil progenitor fate determination (Fig. 7. J. (I)). Further, the splicing factor SF3B1 directly regulates mRNA processing of ELK1 to produce L-ELK1 and S-ELK1, and S-ELK1 was upregulated to replace L-ELK1, pushing uncommitted neutrophil-biased progenitors into neutrophil progenitors in the differentiation of $CD371^{+}$ $CD115^{-}$ GMPs into neutrophil progenitors (Fig. 7. J. (II)-(III)). Taken together, the results indicate that ELK1 is an effective regulatory gene for neutrophil fate determination, and its function is regulated by multiple factors, including the splicing factor SF3B1.

4. Discussion

Neutrophils are well-known to be derived from GMPs. Although mouse neutrophil progenitors have been found in GMPs [4] and the absence of CEBPE causes neutrophil deficiency *in vivo* [40], neither CEBPE mutation [55] nor knockdown results in the disappearance of human neutrophils. Additionally, intravenous immunoglobulin regulates the survival of human but not mouse neutrophils [60]. All these studies show that there exists a difference in the differentiation and function of human and mouse neutrophils. Recently, neutrophil uni-potential progenitors have been identified in fetal bone marrow as Lin^{-} $CD15^{low/+}$ $CD66b^{+}$ SSC^{low} $CD49d^{+}$ [4] or as Lin^{-} $CD66b^{+}$ in adult bone marrow [5]. Excluding $CD371^{high}CD64^{high}$ [32]and $CD64^{high}$ $CD115^{+}$ cells [6] from the GMPs would improve the percentage of progenitors holding neutrophil potential. Here we established an inducible neutrophil differentiation by ALA and dissected the process of neutrophil lineage differentiation from cord blood $CD371^{+}CD115^{-}$ GMPs (contains both the Lin^{-} $CD64^{dim}$ $CD115^{-}$ $CD34^{+}$ $CD45RA^{+}$ NCPs [6] and GMDP [61]). Although MPO, ELANE, PRTN3 and ELANE are upregulated in the reported NCPs [6] and NbPs (Supplementary Fig. 8), these genes are not the neutrophil lineage early cell fate decision genes.

Post-transcriptional modification is widely reported to influence cell metabolism and cell fate [62], such as the mitochondrial metabolism drives erythropoiesis [63] and post-transcriptional networks regulating the transition of myeloblasts to monocytes [9]. In addition, alternative splicing has been reported to play important roles in regulating erythropoiesis [10], granulopoiesis [11], and monocyte-to-macrophage differentiation [64]. In our study, single-cell transcriptome analysis revealed that the transcriptomes of ENbPs and GMPs are more similar than that of MoPs. Most DEGs in ENbPs relative to those in GMPs were RNA binding and RNA splicing-related genes, suggesting that neutrophil maturation could be controlled by post-transcriptional, post--translational, or metabolic regulation. Using the ALA-induced neutrophil deficiency model, we found that ALA significantly changed RNA splicing signals. Based on this analysis, we demonstrated that the critical signal in neutrophil commitment is SF3B1-regulated splicing of ELK1 isoforms to balance neutrophil and monocyte differentiation, with the short isoform regulating neutrophil differentiation and the long isoform regulating monocyte differentiation.

Prior reports have demonstrated that different isoforms of ELK1 have opposite roles in neuronal differentiation [65]. The present study identified differential roles for L-ELK1 and S-ELK1 in the neutrophil commitment. Both L-ELK1 and S-ELK1 played important roles in the commitment of neutrophil progenitors. Normally, ELK1 is required for GMPs to differentiate into neutrophil biased progenitors. Overexpression of L-ELK1 or S-ELK1 increases the production of $CD15^{+}$ $CD66b^{-}$ late neutrophil-biased progenitors derived from $CD371^{+}$ $CD15^{-}$ NbP1 cells. However, overexpression of L-ELK1 impeded differentiation of $CD115^{-}$ $CD15^{+}$ neutrophil-biased progenitors into $CD15^{+}$ $CD66b^{+}$ neutrophil progenitors, while knocking down L-ELK1 enhanced differentiation of $CD115^{-}$ $CD15^{+}$ neutrophil-biased progenitors into $CD15^{+}$ $CD66b^{+}$ neutrophil progenitors.

Numerous prior studies have demonstrated that SF3B1 has critical functions in hematopoiesis, such as myeloid differentiation [66] and erythropoiesis [67], and SF3B1 mutations are commonly detected in MDS (myelodysplastic syndromes) [68]. However, the function of SF3B1 in neutrophil lineage commitment has not been reported. In the present study, we identified that SF3B1 directly binds ELK1 RNA to regulate the generation of L-EKL1 and S-ELK1, balancing neutrophil and monocyte differentiation. SF3B1 knockdown down-regulates L-ELK1 and up-regulates S-ELK1 to enhance neutrophil differentiation. Thus, ELK1 is a critical SF3B1 target for regulation of myeloid differentiation in GMPs.

As previous reports show that upregulation of ELK1 promotes the progression of cervical cancer [69], pancreatic cancer [70], thyroid

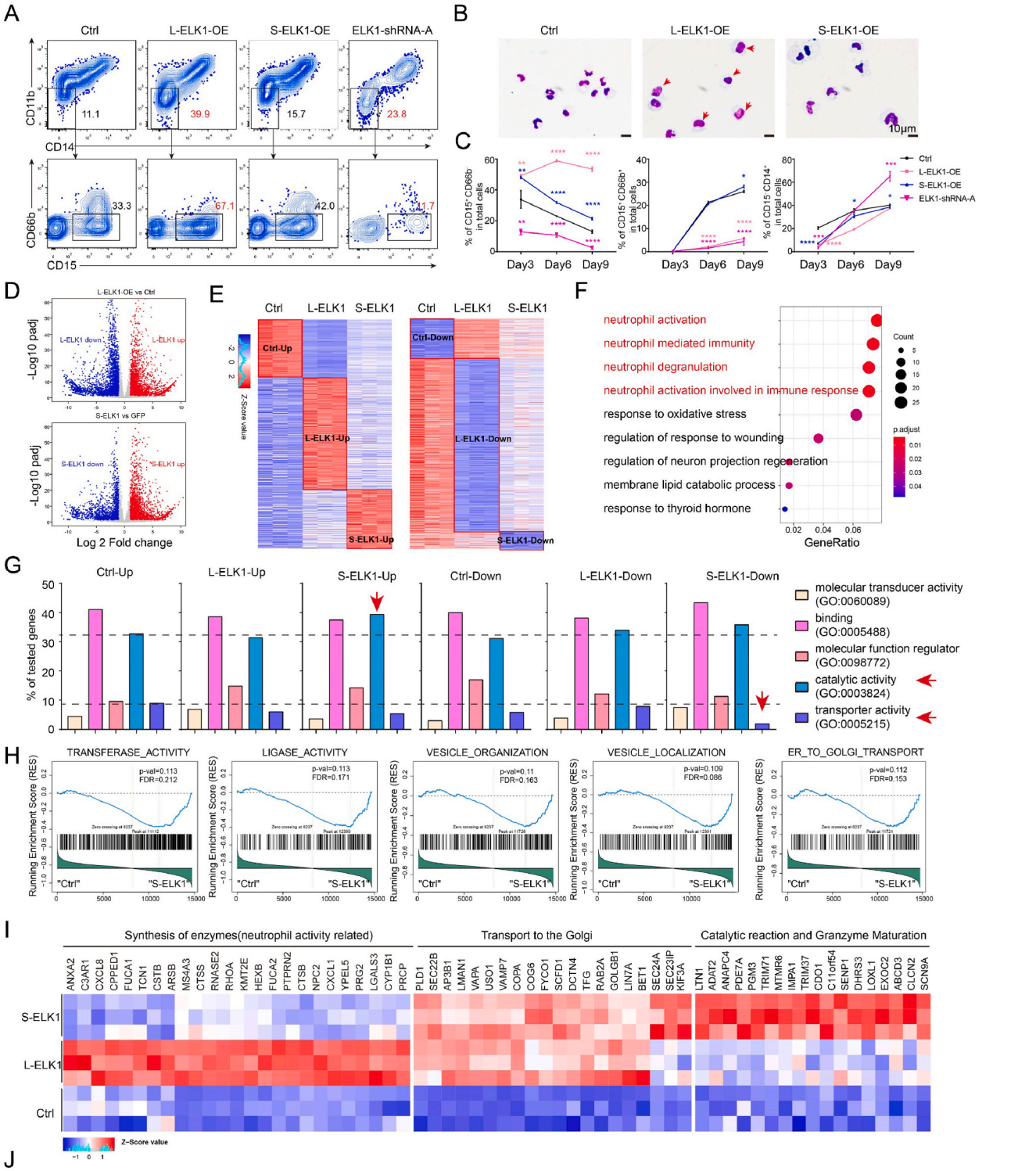

(caption on next page)

Fig. 7. L-ELK1 and S-ELK1 play different roles in neutrophil commitment.
(A) Representative flow cytometry plots of $CD15^+$ $CD66b^+$ neutrophils and $CD15^+$ $CD66b^-$ neutrophil progenitors derived from Ctrl (GFP empty vector), L-ELK1 overexpression (L-ELK1-OE), S-ELK1 overexpression (S-ELK1-OE), and ELK1-shRNA-A viruses transduced NbP1 progenitors. Flow cytometry was performed on day 9 of culture.
(B) Giemsa staining of the morphology of $CD14^-$ $CD15^+$ cells derived from L-ELK1- and S-ELK1-overexpressing NbP1 progenitors on day 9. Arrows indicate immature neutrophil progenitors. Scale bar = 10 μm **(C)** Regular analysis of $CD15^-$ $CD66b^-$, $CD15^+$ $CD66b^+$, and $CD15^-$ $CD14^+$ expression percentages derived from Ctrl (GFP empty vector), L-ELK1 overexpression, S-ELK1 overexpression, and ELK1-shRNA-A knockdown viruses transduced NbP1 progenitors.
(D) Volcano plots were used to analyze differential expression of genes in Ctrl, L-ELK1- and S-ELK1-overexpressing NbP1 progenitors.
(E) Heatmaps presenting upregulated and downregulated gene sets in Ctrl-, L-ELK1-, and S-ELK1-overexpressing NbP1 progenitors.
(F) GO enrichment analysis of the L-ELK1-specific upregulated genes.
(G) Gene ontology category analysis of specific upregulated and downregulated gene sets in Ctrl-, L-ELK1- and S-ELK1-overexpressing NbP1 progenitors. Gene ontology category analysis was performed using http://www.pantherdb.org/.
(H) GSEA was used to analyze signal changes in S-ELK1-overexpressing NbP1 progenitors.
(I) Heatmaps present the L-ELK1- and S-ELK1-upregulated genes related to enzyme synthesis, endoplasmic reticulum to Golgi transport, and enzyme catalytic reaction signals.
(J) Diagram of the marker-changing model in $CD371^+$ $CD115^-$ GMPs differentiating into neutrophil progenitors (I), regulation of the SF3B1-ELK1 signaling axis (II), and the working model of the roles of L-ELK1 and S-ELK1 in the different differentiation stages of neutrophils (III).

cancer [71], colorectal cancer [72] and breast cancer [73], and suppression of ELK1 help to inhibit thyroid cancer [71], pancreatic cancer [74], breast cancer [75] and cervical cancer [76]. ALA has been applied to cancer therapy in multiple cancers [77], but it's unclear how ALA suppress cancer progression. Our founding might help to explain the mechanism of cancer therapy using ALA. And ALA could use to inhibit the progression of the cancers promoted by upregulations of ELK1. In addition, ALA could completely inhibit the neutrophil differentiation derived from hematogenic stem cells, ALA would be applied to inhibit the inflammation in many cases, such as serious inflammation caused by COVID-19.

In summary, the present study provides new insights into the regulatory mechanisms of human neutrophil lineage commitment at post-transcriptional modification by ALA, which can potentially be translated to targeted drug development for MDS, neutrophil regeneration and cancer therapy.

5. Conclusions

Overall, we established an inducible neutrophil differentiation model by using an antioxidant ALA and defined the neutrophil progenitor commitment process from $CD371^+$ $CD115^-$ GMPs by CD34 and CD15. Moreover, we confirmed that the neutrophil transcriptomes of $CD371^+$ $CD115^-$ GMPs, neutrophil-biased progenitors, and monocyte progenitors had similar developmental characteristics both *in vivo* and *in vitro*. Sequentially, we discovered that ELK1 was essential for human neutrophil lineage determination, SF3B1 regulated RNA splicing of L-ELK1 and L-ELK1 increased genes related to enzyme synthesis and endoplasmic reticulum to Golgi transport while S-ELK1 upregulated additional genes related to endoplasmic reticulum to Golgi transport catalytic reactions, and enzyme maturation-related genes.

Author contributions

Yong Dong conceived, initialed, and designed this project. Yong Dong and Yimeng Zhang collected all the data. Yong Dong analyzed and interpreted all the data analysis. Yongping Zhang collected the human BM. Zhenyang Lai and Qiang Chen provided cord blood. Xu Pan and Yijin Chen performed cell sorting, Ju Bai, Ya Zhou, Qiongxiu Zhou, Yonggang Zhang provided help in this research. Yong Dong, Yimeng Zhang and Feng Ma discussed the data and wrote the manuscript. Feng Ma approved the manuscript.

Funding

This research is supported by the China Postdoctoral Fund Program (grant number 2018M641265), the CAMS Initiatives for Innovative Medicine (2019-I2M-1–006, 2017-I2M−2005, 2019-RC-HL-016), the grant from the National Natural Science Foundation of China (grant number 82000119, 82170121), and the Disciplinary Construction Innovation Team Foundation of Chengdu Medical College (grant number CMC-XK-2102).

Availability of data and materials

All data generated or analyzed during this study are included in this published article.

Declaration of competing interest

The authors declare that they have no known competing financial interests or personal relationships that could have appeared to influence the work reported in this paper.

Acknowledgments

We thank professor Jinyong Wang for providing PCCL, PLP1 and PLP2 overexpression vectors.

Appendix A. Supplementary data

Supplementary data to this article can be found online at https://doi.org/10.1016/j.redox.2022.102392.

Abbreviations

ALA	Alpha lipoic acid
HSC	Hematopoietic stem cell
HPSC	Hematopoietic stem and progenitor cell
GMP	Granulocyte-monocyte progenitor
CMP	Common myeloid progenitor
MEP	Megakaryocyte-erythrocyte progenitor
NbP	Neutrophil-biased progenitor
ENbP	Early neutrophil-biased progenitor
LNbP	Late neutrophil-biased progenitor
ELK1	ETS domain-containing protein Elk-1
SF3B1	Splicing factor 3b, subunit 1
SCF	Stem cell factor
IL-3	Interleukin-3
IL-6	Interleukin-6
TPO	Thrombopoietin
EPO	Erythropoietin
FLT3L	FMS-like tyrosine kinase-3 ligand
G-CSF	Granulocyte colony stimulating factor
GM-CSF	Granulocyte-macrophage colony stimulating factor
ROS	Reactive oxygen species

LSK	Lin (CD2, CD3, CD4, CD8, CD11b, B220, Ter19, Mac1)$^-$ Sca1$^+$ ckit$^+$
BM	Bone marrow
MDS	Myelodysplastic syndromes
NAC	N-Acetyl-L-cysteine
NAD	N-Acetyl-D-cysteine
VC	L-Ascorbic acid (Vitamin C)
VE	α-Vitamin E
GSH	L-Glutathione reduced

References

[1] D.C. Dale, How I diagnose and treat neutropenia, Curr. Opin. Hematol. 23 (1) (2016) 1–4.
[2] A.A. Marfin, T.H. Price, Granulocyte transfusion therapy, J. Intensive Care Med. 30 (2) (2015) 79–88.
[3] J.A. Cancelas, Granulocyte transfusion: questions remain, Blood 126 (18) (2015) 2082–2083.
[4] I. Kwok, et al., Combinatorial Single-Cell Analyses of Granulocyte-Monocyte Progenitor Heterogeneity Reveals an Early Uni-Potent Neutrophil Progenitor, Immunity, 2020.
[5] H.Q. Dinh, et al., Coexpression of CD71 and CD117 identifies an early unipotent neutrophil progenitor population in human bone marrow, Immunity 53 (2) (2020) 319–334 e6.
[6] F. Calzetti, et al., CD66b(-)CD64(dim)CD115(-) cells in the human bone marrow represent neutrophil-committed progenitors, Nat. Immunol. 23 (5) (2022) 679–691.
[7] R. Drissen, et al., Identification of two distinct pathways of human myelopoiesis, Sci Immunol 4 (35) (2019).
[8] L.G. Ng, R. Ostuni, A. Hidalgo, Heterogeneity of neutrophils, Nat. Rev. Immunol. 19 (4) (2019) 255–265.
[9] G. Fontemaggi, et al., Identification of post-transcriptional regulatory networks during myeloblast-to-monocyte differentiation transition, RNA Biol. 12 (7) (2015) 690–700.
[10] C.R. Edwards, et al., A dynamic intron retention program in the mammalian megakaryocyte and erythrocyte lineages, Blood 127 (17) (2016) e24–e34.
[11] J.J. Wong, et al., Orchestrated intron retention regulates normal granulocyte differentiation, Cell 154 (3) (2013) 583–595.
[12] B. Ye, et al., Induction of Functional Neutrophils from Mouse Fibroblasts by Thymidine through Enhancement of Tet3 Activity, Cell Mol Immunol, 2022.
[13] A. Solmonson, R.J. DeBerardinis, Lipoic acid metabolism and mitochondrial redox regulation, J. Biol. Chem. 293 (20) (2018) 7522–7530.
[14] H. Moini, L. Packer, N.E. Saris, Antioxidant and prooxidant activities of alpha-lipoic acid and dihydrolipoic acid, Toxicol. Appl. Pharmacol. 182 (1) (2002) 84–90.
[15] D. Xia, et al., Alpha lipoic acid inhibits oxidative stress-induced apoptosis by modulating of Nrf2 signalling pathway after traumatic brain injury, J. Cell Mol. Med. 23 (6) (2019) 4088–4096.
[16] M. Rahimifard, et al., Multiple protective mechanisms of alpha-lipoic acid in oxidation, apoptosis and inflammation against hydrogen peroxide induced toxicity in human lymphocytes, Mol. Cell. Biochem. 403 (1–2) (2015) 179–186.
[17] Y. Li, et al., Alpha lipoic acid protects lens from H(2)O(2)-induced cataract by inhibiting apoptosis of lens epithelial cells and inducing activation of anti-oxidative enzymes, Asian Pac. J. Trop. Med. 6 (7) (2013) 548–551.
[18] J. Tripathy, et al., alpha-Lipoic acid inhibits the migration and invasion of breast cancer cells through inhibition of TGFbeta signaling, Life Sci. 207 (2018) 15–22.
[19] P. Peng, et al., Alpha-lipoic acid inhibits lung cancer growth via mTOR-mediated autophagy inhibition, FEBS Open Bio 10 (4) (2020) 607–618.
[20] M.J. Jeon, et al., Alpha lipoic acid inhibits proliferation and epithelial mesenchymal transition of thyroid cancer cells, Mol. Cell. Endocrinol. 419 (2016) 113–123.
[21] Y. Dong, et al., Alpha lipoic acid promotes development of hematopoietic progenitors derived from human embryonic stem cells by antagonizing ROS signals, J. Leukoc. Biol. (2020).
[22] C. Wambi, et al., Dietary antioxidants protect hematopoietic cells and improve animal survival after total-body irradiation, Radiat. Res. 169 (4) (2008) 384–396.
[23] N. Ramakrishnan, W.W. Wolfe, G.N. Catravas, Radioprotection of hematopoietic tissues in mice by lipoic acid, Radiat. Res. 130 (3) (1992) 360–365.
[24] H.J. Kwak, et al., Myeloid cell-derived reactive oxygen species externally regulate the proliferation of myeloid progenitors in emergency granulopoiesis, Immunity 42 (1) (2015) 159–171.
[25] S. Saha, S.K. Biswas, Tumor-Associated neutrophils show phenotypic and functional divergence in human lung cancer, Cancer Cell 30 (1) (2016) 11–13.
[26] B. Mao, et al., Early development of definitive erythroblasts from human pluripotent stem cells defined by expression of glycophorin A/CD235a, CD34, and CD36, Stem Cell Rep. 7 (5) (2016) 869–883.
[27] T. Wang, et al., Trim27 confers myeloid hematopoiesis competitiveness by up-regulating myeloid master genes, J. Leukoc. Biol. 104 (4) (2018) 799–809.
[28] F. Tang, et al., RNA-Seq analysis to capture the transcriptome landscape of a single cell, Nat. Protoc. 5 (3) (2010) 516–535.
[29] N. Meng, et al., Small protein hidden in lncRNA LOC90024 promotes "cancerous" RNA splicing and tumorigenesis, Adv. Sci. 7 (10) (2020), 1903233.
[30] S. Hou, L. Shi, H. Lei, Biotin-streptavidin affinity purification of RNA-protein complexes assembled in vitro, Methods Mol. Biol. 1421 (2016) 23–34.
[31] J. Olweus, P.A. Thompson, F. Lund-Johansen, Granulocytic and monocytic differentiation of CD34hi cells is associated with distinct changes in the expression of the PU.1- regulated molecules, CD64 and macrophage colony-stimulating factor receptor, Blood 88 (10) (1996) 3741–3754.
[32] S. Kawamura, et al., Identification of a human clonogenic progenitor with strict monocyte differentiation potential: a counterpart of mouse cMoPs, Immunity 46 (5) (2017) 835–848 e4.
[33] M. Zhang, et al., Transcription factor Hoxb5 reprograms B cells into functional T lymphocytes, Nat. Immunol. 19 (3) (2018) 279–290.
[34] C. Gemelli, et al., Virally mediated MafB transduction induces the monocyte commitment of human CD34+ hematopoietic stem/progenitor cells, Cell Death Differ. 13 (10) (2006) 1686–1696.
[35] Louise M. Kelly, U.E. Isabelle Lafon, Michael H. Sieweke1, Thomas Graf2, MafB Is an Inducer of Monocytic Differentiation, 2000.
[36] S.P. Hegde, et al., c-Maf induces monocytic differentiation and apoptosis in bipotent myeloid progenitors, Blood 94 (5) (1999) 1578–1589.
[37] N.A. Fischbach, et al., HOXB6 overexpression in murine bone marrow immortalizes a myelomonocytic precursor in vitro and causes hematopoietic stem cell expansion and acute myeloid leukemia in vivo, Blood 105 (4) (2005) 1456–1466.
[38] U. Cytlak, et al., Differential IRF8 transcription factor requirement defines two pathways of dendritic cell development in humans, Immunity 53 (2) (2020) 353–370, e8.
[39] D. Kurotaki, et al., IRF8 inhibits C/EBPalpha activity to restrain mononuclear phagocyte progenitors from differentiating into neutrophils, Nat. Commun. 5 (2014) 4978.
[40] M. Evrard, et al., Developmental analysis of bone marrow neutrophils reveals populations specialized in expansion, trafficking, and effector functions, Immunity 48 (2) (2018) 364–379 e8.
[41] D.V. Grigorieva, et al., Myeloperoxidase stimulates neutrophil degranulation, Bull. Exp. Biol. Med. 161 (4) (2016) 495–500.
[42] J. Ahmad, et al., Physics-driven identification of clinically approved and investigation drugs against human neutrophil serine protease 4 (NSP4): a virtual drug repurposing study, J. Mol. Graph. Model. 101 (2020), 107744.
[43] A.J. Sawyer, et al., Transcriptomic profiling identifies neutrophil-specific upregulation of cystatin F as a marker of acute inflammation in humans, Front. Immunol. 12 (2021).
[44] A. Gatti, et al., Quantification of neutrophil and monocyte CD64 expression: a predictive biomarker for active tuberculosis, Int. J. Tubercul. Lung Dis. 24 (2) (2020) 196–201.
[45] L.J. Druhan, et al., Leucine rich alpha-2 glycoprotein: a novel neutrophil granule protein and modulator of myelopoiesis, PLoS One 12 (1) (2017), e0170261.
[46] M. Barrett, Immunolocalization of human cystatins in neutrophils and lymphocytes, Histochemistry 80 (1984) 373–377.
[47] Christophe Perrina, et al., Expression of LSLCL, a new C-type lectin, is closely restricted, in bone marrow, to immature neutrophils, C R Acad. Sci. III 324 (2001) 1125–1132.
[48] David R. Greaves, et al., CCR6, a CC chemokine receptor that interacts with macrophage inflammatory protein 3a and is highly expressed in human dendritic cells, J. Exp. Med. 186 (6) (1997) 837–844.
[49] L. Heger, et al., CLEC10A is a specific marker for human CD1c+ dendritic cells and enhances their toll-like receptor 7/8-induced cytokine secretion, Front. Immunol. 9 (2018).
[50] C. Angénieux, et al., The Cellular Pathway of CD1e in Immature and Maturing Dendritic Cells, Traffic 6 (4) (2005) 286–302.
[51] E.J. Ryan, et al., Ligation of dendritic cell–associated lectin–1 induces partial maturation of human monocyte derived dendritic cells, Hum. Immunol. 70 (1) (2009) 1–5.
[52] B. Jahrsdörfer, et al., Granzyme B produced by human plasmacytoid dendritic cells suppresses T-cell expansion, Blood 115 (6) (2010) 1156–1165.
[53] Petr Danek, et al., beta-Catenin-TCF/LEF Signaling Promotes Steady-State and Emergency Granulopoiesis via G-CSF Receptor Upregulation, blood, 2020.
[54] J. Yang, et al., Histone modification signature at myeloperoxidase and proteinase 3 in patients with anti-neutrophil cytoplasmic autoantibody-associated vasculitis, Clin. Epigenet. 8 (2016) 85.
[55] N.K. Serwas, et al., CEBPE-mutant specific granule deficiency correlates with aberrant granule organization and substantial proteome alterations in neutrophils, Front. Immunol. 9 (2018) 588.
[56] B. Garg, et al., Inducible expression of a disease-associated ELANE mutation impairs granulocytic differentiation, without eliciting an unfolded protein response, J. Biol. Chem. (2020).
[57] C. Perrin, et al., Expression of LSLCL, a new C-type lectin, is closely restricted, in bone marrow, to immature neutrophils, C R Acad. Sci. III 324 (12) (2001) 1125–1132.
[58] L. Bencheikh, et al., Dynamic gene regulation by nuclear colony-stimulating factor 1 receptor in human monocytes and macrophages, Nat. Commun. 10 (1) (2019) 1935.
[59] S. Schmeier, et al., Deciphering the transcriptional circuitry of microRNA genes expressed during human monocytic differentiation, BMC Genom. 10 (2009) 595.
[60] C. Schneider, et al., IVIG regulates the survival of human but not mouse neutrophils, Sci. Rep. 7 (1) (2017) 1296.
[61] J. Lee, et al., Restricted dendritic cell and monocyte progenitors in human cord blood and bone marrow, J. Exp. Med. 212 (3) (2015) 385–399.
[62] O.A. Tarazona, O. Pourquie, Exploring the influence of cell metabolism on cell fate through protein post-translational modifications, Dev. Cell 54 (2) (2020) 282–292.

[63] M.P. Rossmann, et al., Cell-specific transcriptional control of mitochondrial metabolism by TIF1gamma drives erythropoiesis, Science 372 (6543) (2021) 716–721.
[64] H. Liu, et al., Alternative splicing analysis in human monocytes and macrophages reveals MBNL1 as major regulator, Nucleic Acids Res. 46 (12) (2018) 6069–6086.
[65] P. Vanhoutte, et al., Opposing roles of Elk-1 and its brain-specific isoform, short Elk-1, in nerve growth factor-induced PC12 differentiation, J. Biol. Chem. 276 (7) (2001) 5189–5196.
[66] S.A. Mian, et al., SF3B1 mutant MDS-initiating cells may arise from the haematopoietic stem cell compartment, Nat. Commun. 6 (1) (2015).
[67] Y. Huang, et al., SF3B1 deficiency impairs human erythropoiesis via activation of p53 pathway: implications for understanding of ineffective erythropoiesis in MDS, J. Hematol. Oncol. 11 (1) (2018).
[68] K.S. Luca Malcovati, et al., SF3B1-mutant MDS as a distinct disease subtype: a proposal from the International Working Group for the Prognosis of MDS, Blood 136 (2) (2020) 157–170.
[69] Q. Tang, et al., Circular RNA hsa_circ_0000515 acts as a miR-326 sponge to promote cervical cancer progression through up-regulation of ELK1, Aging (Albany NY) 11 (22) (2019) 9982–9999.
[70] Q. Yan, et al., ELK1 enhances pancreatic cancer progression via LGMN and correlates with poor prognosis, Front. Mol. Biosci. 8 (2021), 764900.
[71] Y. Kong, et al., Suppression of Elk1 inhibits thyroid cancer progression by mediating PTEN expression, Oncol. Rep. 40 (3) (2018) 1769–1776.
[72] J. Ma, et al., c-KIT-ERK1/2 signaling activated ELK1 and upregulated carcinoembryonic antigen expression to promote colorectal cancer progression, Cancer Sci. 112 (2) (2021) 655–667.
[73] S. Wang, et al., ELK1-induced up-regulation of KIF26B promotes cell cycle progression in breast cancer, Med. Oncol. 39 (1) (2021) 15.
[74] S. Li, et al., miR-597-5p inhibits cell growth and promotes cell apoptosis by targeting ELK1 in pancreatic cancer, Hum. Cell 33 (4) (2020) 1165–1175.
[75] A. Ahmad, et al., Tumor-suppressive miRNA-135a inhibits breast cancer cell proliferation by targeting ELK1 and ELK3 oncogenes, Gene. Genomic. 40 (3) (2018) 243–251.
[76] W. Zhang, S. Zhang, Downregulation of circRNA_0000285 suppresses cervical cancer development by regulating miR197-3p-ELK1 Axis, Cancer Manag. Res. 12 (2020) 8663–8674.
[77] L. Novotny, P. Rauko, C. Cojocel, alpha-Lipoic acid: the potential for use in cancer therapy, Neoplasma 55 (2) (2008) 81–86.